EBioMedicine 30 (2018) 38–51

Contents lists available at ScienceDirect

EBioMedicine

journal homepage: www.ebiomedicine.com

Research Paper

# Endogenous Mobilization of Bone-Marrow Cells Into the Murine Retina Induces Fusion-Mediated Reprogramming of Müller Glia Cells

Martina Pesaresi [a,b,1], Sergi A. Bonilla-Pons [a,b,c,1], Giacoma Simonte [a,b,1], Daniela Sanges [a,b], Umberto Di Vicino [a,b], Maria Pia Cosma [a,b,d,*]

[a] Center for Genomic Regulation (CRG), The Barcelona Institute of Science and Technology, Barcelona, Spain
[b] Universitat Pompeu Fabra (UPF), Barcelona, Spain.
[c] Universitat de Barcelona (UB), Barcelona, Spain.
[d] ICREA, Barcelona, Spain.

ARTICLE INFO

*Article history:*
Received 6 June 2017
Received in revised form 2 February 2018
Accepted 26 February 2018
Available online 28 February 2018

*Keywords:*
Retinal damage
NMDA-damage
Müller glial cells
Cell fusion-mediated reprogramming
Bone-marrow cells
Endogenous migration
SDF1/CXCR4 pathway

ABSTRACT

Müller glial cells (MGCs) represent the most plastic cell type found in the retina. Following injury, zebrafish and avian MGCs can efficiently re-enter the cell cycle, proliferate and generate new functional neurons. The regenerative potential of mammalian MGCs, however, is very limited. Here, we showed that *N*-methyl-D-aspartate (NMDA) damage stimulates murine MGCs to re-enter the cell cycle and de-differentiate back to a progenitor-like stage. These events are dependent on the recruitment of endogenous bone marrow cells (BMCs), which, in turn, is regulated by the stromal cell-derived factor 1 (SDF1)-C-X-C motif chemokine receptor type 4 (CXCR4) pathway. BMCs mobilized into the damaged retina can fuse with resident MGCs, and the resulting hybrids undergo reprogramming followed by re-differentiation into cells expressing markers of ganglion and amacrine neurons. Our findings constitute an important proof-of-principle that mammalian MGCs retain their regenerative potential, and that such potential can be activated via cell fusion with recruited BMCs. In this perspective, our study could contribute to the development of therapeutic strategies based on the enhancement of mammalian endogenous repair capabilities.



## 1. Introduction

Müller glia cells (MGCs) are the main glial cell type of the retina, where they fulfill typical functions of glia in the brain. In particular, they are responsible for the maintenance of retinal structure; they also actively participate in the regulation of ion homeostasis and in neurotransmitter recycling (Bringmann et al., 2009; Reichenbach and Bringmann, 2013; Newman and Reichenbach, 1996). Additionally, MGCs can act as adult stem cells, especially in early vertebrates such as teleost fish (Lenkowski and Raymond, 2014; Nagashima et al., 2013), but also in chicken (Fischer and Reh, 2001, 2003; Gallina et al., 2016). In these animals, MGCs respond to injury by reactivating expression of retinal stem cell genes. Like retinal progenitor cells, they re-enter the cell cycle, proliferate, and eventually re-differentiate into functional retinal neurons (Thummel et al., 2008; Fausett and Goldman, 2006; Fischer and Reh, 2001, 2002). Following pharmacological damage of either ganglion or photoreceptor cells, adult murine MGCs can also re-enter the cell cycle and contribute to neuronal regeneration (Karl et al., 2008; Wan et al., 2008; Ooto et al., 2004; Todd et al., 2015). However, the frequency of such events is extremely low. As a consequence, proliferative MGCs are unable to fully rescue retinal functionality (Karl and Reh, 2010).

The reasons underlying limited regenerative potential of MGCs in mammals have not been clearly elucidated yet. However, a number of studies have identified some of the key events that could contribute to the enhancement of endogenous mammalian regeneration. In particular, proliferation of murine MGCs can be stimulated by overexpression of Ascl1, a transcription factor essential during retinal development (Pollak et al., 2013). Pharmacological perturbation of specific signaling pathways can also stimulate the neural regenerative potential of mammalian MGCs; these include, for instance, Wnt/β-catenin, EGF, FGF, and insulin pathways (Karl et al., 2008; Osakada et al., 2007; Close et al., 2006; Todd et al., 2015; Ooto et al., 2004; Tao et al., 2016; Yao et al., 2016).

Furthermore, we have previously shown that MGCs can undergo de-differentiation and re-entry into the cell cycle following fusion with transplanted hematopoietic stem and progenitor cells (HSPCs) (Sanges et al., 2013, 2016). Importantly, fusion events are largely damage-dependent and result in the formation of tetraploid BM-derived

* Corresponding author at: Center for Genomic Regulation (CRG), C/Dr. Aiguader, 88 08003 Barcelona, Spain.
*E-mail address:* pia.cosma@crg.es (M.P. Cosma).
[1] These authors contributed equally to this work.

https://doi.org/10.1016/j.ebiom.2018.02.023

hybrids. Interestingly, the reprogramming efficiency of newly generated hybrids is significantly increased when the Wnt/β-catenin pathway is activated in the HSPCs prior to transplantation (Sanges et al., 2013, 2016).

Bone-marrow cells (BMCs, including HSPCs) have been extensively shown to contribute to the repair of damaged tissues and organs (Wang et al., 2003; Orlic et al., 2001; Weimann et al., 2003b; Lagasse et al., 2000; Kale et al., 2003; Jackson et al., 2001). This can be attributed to their plasticity and their ability to change identity via either transdifferentiation or cell fusion-mediated events. In particular, endogenous BMCs have been shown to fuse with several cell types, including glia (Altarche-Xifro et al., 2016), neurons (Johansson et al., 2008; Alvarez-Dolado et al., 2003), hepatocytes (Vassilopoulos et al., 2003; Pedone et al., 2017), cardiomyocytes (Nygren et al., 2004), and gut cells (Rizvi et al., 2006; Davies et al., 2009).

Changes in cellular identity are intimately coupled to the recruitment of BMCs to the site of damage. Several cytokines have been proposed to facilitate BMC recruitment. Among these, stromal-derived factor 1 (SDF1, also known as C-X-C motif chemokine 12 - CXCL12) seems to play a crucially important role (Cheng and Qin, 2012; Nervi et al., 2006; Aiuti et al., 1997).

SDF1 specifically binds to the C-X-C motif chemokine receptor type 4 (CXCR4). The SDF1/CXCR4 signaling axis has already been extensively implicated in the regulation of BMC homing and mobilization (Nervi et al., 2006; Kollet et al., 2003). Robust mobilization of CXCR4-expressing HSPCs in the peripheral blood occurs when plasma levels of SDF1 are increased (Hattori et al., 2001). Additionally, SDF1 is one of the major players in the regulation of HSPC trans-endothelial migration (Aiuti et al., 1997). Interestingly, SDF1 expression is also strongly up-regulated following damage in several tissues, including the liver, the brain, and the retina (Mocco et al., 2014; Lima E Silva et al., 2007; Pedone et al., 2017).

We decided to use a model of *N*-methyl-D-aspartate (NMDA)-induced excitotoxicity, characterized by apoptosis of ganglion and amacrine neurons (Lucas and Newhouse, 1957; Siliprandi et al., 1992; Sucher et al., 1997). We investigated damage-induced recruitment of endogenous BMCs into the retina, showing its dependence on the activity of the SDF1/CXCR4 pathway. We also showed that NMDA-damage could stimulate MGCs to dedifferentiate, and that such dedifferentiation was the result of fusion events involving MGCs and endogenously mobilized BMCs. Resulting hybrids were found to contribute to the replacement of damaged neurons, generating calretinin-positive ganglion and amacrine cells.

Overall, our data suggests that cell fusion is one of the mechanisms underlying MGC plasticity. MGC ability to de-differentiate and proliferate is strongly dependent on the recruitment of their fusion partners, endogenous BMCs. Migration of BMCs is, in turn, regulated by the SDF1/CXCR4 signaling axis. As a result, modulation of the SDF1/CXCR4 pathway can affect MGC plasticity, and the extent to which MGCs can contribute to regeneration of damaged retinal tissue.

## 2. Materials and Methods

### 2.1. Animal Care and Treatment

Mice were maintained under a 12-h light/dark cycle with access to food and water *ad libitum*, in accordance with the Ethical Committee for Animal Experimentation (CEEA) of the Government of Catalonia. The CEEA of the Parc de Recerca Biomèdica de Barcelona (PRBB, Spain) reviewed and approved all animal procedures. Additionally, procedures and experiments were performed in accordance with the ARVO Statement for the Use of Animals in Ophthalmic and Vision Research, and with ARRIVE (Animal Research: Reporting of In Vivo Experiments) guidelines (Kilkenny et al., 2011).

Male and female animals between 8 and 12 weeks were used for the study. They were assigned randomly to the various treatment groups. A minimum of three mice per treatment group was used. General anesthesia was induced when needed with intraperitoneal injection of ketamine (70 mg/kg) and medetomidine (10 mg/kg). Anesthesia was reversed with atipamezole (2 mg/kg). At endpoints, mice were euthanized using $CO_2$.

### 2.2. Transgenic Mouse Lines

We used the following transgenic mouse lines: Vav-Cre (Stadtfeld and Graf, 2005); CAG-RFP (Long et al., 2005); GFAP-Cre (Zhuo et al., 2001); Calr-Cre (Taniguchi et al., 2011); R26Y (B6.129X1-Gt(ROSA)26Sortm1(EYFP)Cos/J) (Srinivas et al., 2001).

Additionally, we generated GFAP-Cre/R26Y and Calr-Cre/R26Y mice. These strains were generated by crossing R26Y mice with either GFAP-Cre or Calr-Cre ones. As a result, mice possessed both the Rosa 26-LoxP-stop-LoxP-YFP [R26Y] transgene and either the GFAP-Cre or the Calr-Cre transgene.

### 2.3. Sub-lethal Irradiation and Bone Marrow Transplantation

Bone marrow (BM) transplantation was carried out as previously reported (Fazel et al., 2006). Briefly, 8–12 weeks-old mice received total body irradiation with 9 Gγ (double dose of 4,5 Gγ) six weeks prior to retinal damage and/or drug treatment. 3–4 h after irradiation, they received an intravenous injection of $1 \times 10^7$ BM cells from young donor mice. Total BM cells were obtained by gently flushing femurs and tibias with PBS.

R26Y/BM$^{CRE\text{-}RFP}$ chimeric animals were generated by replacing the BM of transgenic mice carrying the R26Y allele with the BM of CAG-RFP/Vav-Cre donor mice.

GFAP-Cre/BM$^{R26Y}$ chimeric mice were generated by replacing the BM of GFAP-Cre mice with the BM of donor transgenic mice carrying the R26Y allele.

Calr-Cre/R26Y/BM$^{RFP}$ mice were generated by replacing the BM of Calr-Cre/R26Y mice with that of donor CAG-RFP mice.

### 2.4. Retinal Damage and Drug Treatment

Mice were anaesthetized and intravitreally injected with 2 μl of either NMDA (20 mmol/μl; Sigma) or PBS, as a control. Briefly, a 30-G needle was used to carefully make a small incision at the upper temporal ora serrata. The 33-gauge needle of a Hamilton's syringe was then inserted into the incision to inject PBS or NMDA into the vitreous. The needle was left in place for 10 s before being retracted to avoid reflux. Eye samples were isolated 24 h (24 hpi), 4 days (4 dpi) or 3 weeks (3 wpi) post-injection.

To investigate the effects of SDF1/CXCR4 signaling modulation, we intravitreally injected 1 μl of SDF1 (50 ng/μl, Sigma) immediately after PBS or NMDA treatment. Control eyes were injected with an equivalent volume of PBS. To block migration of bone marrow cells, mice received intraperitoneal injections of the CXCR4 antagonist AMD3100 (1 mg/kg, Sigma A5602). AMD3100 injections were performed every 24 h and for a maximum of three consecutive days, starting the same day of the NMDA treatment (a single injection for mice sacrificed at 24 hpi, and three injections in total for mice sacrificed either 4 dpi or 3 wpi).

### 2.5. FACS Sorting of Müller Glia Cells and Hybrids for Gene Expression Analysis

For FACS analysis and sorting, retinae were dissected from the enucleated eyes and disaggregated in trypsin for 20–30 min at 37 °C. Retinal samples were then mechanically triturated, filtered, pelleted, and resuspended in PBS supplemented with 2% fetal bovine serum (FBS). A solution of 6-diamidino-2-phenylindole (DAPI, Sigma 10236276) was also added to exclude dead cells from the analysis (5 mg/ml, used 1:1′000). Flow cytometry analysis was performed in a LSR Fortessa (Becton

Dickinson) with FACSDiva (Becton Dickinson) software. Cell sorting was performed using the BD FACSAria II sorting machine (Becton Dickinson). For macrophage analysis, we used a rat primary anti-MAC-1 (CD11b) antibody (1:100, eBioscience 17-0112).

### 2.6. RNA Extraction and Real-time PCR

RNA was extracted from sorted cells using either the RNA Isolation Mini kit or the RNA Isolation Micro one (both QIAGEN), according to the manufacturer protocol. RNA was reverse-transcribed with SuperScript III (Invitrogen). Real-time PCR reactions were performed using Platinum SYBR green qPCR SuperMix-UDG (Invitrogen) in a LyghtCycler 480 (Roche) machine, according to the manufacturer recommendations. The oligos used are listed in supplementary table S1. The cycling conditions were as follows: (1) denaturation [1 cycle, 95 °C for 5 min, ramp rate (°C/s) = 4.4 °C]; (2) amplification [45 cycles: 95 °C for 10s, ramp rate (°C/s) = 4.4 °C; 60 °C for 10s, ramp rate (°C/s) = 2.2 °C; 72 °C for 15 s, ramp rate (°C/s) = 4.4°]; (3) melting [1 cycle: 95 °C for 10s, ramp rate (°C/s) = 4.4 °C; 62 °C for 10s, ramp rate (°C/s) = 2.2 °C; 97 °C, ramp rate (°C/s) = 0.07 °C, acquisitions (per °C) = 8]; (4) cooling [1 cycle, 40 °C, ramp rate (°C/s) = 1.5 °C].

RT-PCR data was normalized to *Gapdh* expression. We averaged at least three independent experiments, and, for each sample, we had at least a technical duplicate. Relative mRNA levels were presented as fold-changes with respect to the appropriate control.

### 2.7. Fixing, Sectioning, Immunohistochemistry and Immuno-TUNEL

Eyes were enucleated and fixed by immersion in 4% paraformaldehyde (PFA) overnight at 4 °C. They were embedded in paraffin the following day. Serial transversal sections of 5 μm of thickness were prepared and processed for immunofluorescence staining. Briefly, sections were de-paraffinized by sequential treatment with Xilene, EtOH 100%, EtOH 95%, EtOH 90%, EtOH 80%, EtOH 70%, EtOH 50% and $H_2O$ (3 washes, 5 min per wash). Slices were placed in a plastic rack with an antigen retrieval buffer (0.1 M NaCitrate and 0.3%Triton X-100 in PBS) and boiled for 4′ in a domestic microwave. After a wash with cold water, sections were blocked in 10% normal goat serum (NGS) for 30 min and in 1% NGS for an additional 30 min. Retinal sections were incubated overnight at 4 °C with primary antibodies diluted in PBS. They were then washed with PBS and incubated with secondary antibodies for 1 h at room temperature.

For retinal flat mount immunostaining, whole retinae were dissected and fixed for 1 h with 4% PFA. They were then permeabilized and blocked (10% NGS, 0.3% Triton X-100 in PBS), prior to incubation with primary antibodies (two consecutive overnights at 4 °C). Retinae were then washed with PBS and incubated with secondary antibodies.

TUNEL staining was performed according to manufacturer's instructions (In Situ Cell Death Detection Kit, Fluorescein). Briefly, retinal flat mounts were permeabilized and blocked (10% NGS, 0.3% Triton X-100 in PBS). They were then incubated with the TUNEL reaction mixture at 37 °C. DAPI was also used to stain for cell nuclei.

For immuno-TUNEL staining, we first performed immunostaining with primary antibodies, as described above. We then proceeded with the TUNEL reaction, and, lastly, with the secondary antibody staining.

The list of primary antibodies used for both retinal flat mounts and sections can be found in Table S2. We used the following secondary antibodies: anti-chicken Alexa Fluor 488, anti-mouse Alexa Fluor 568, anti-rabbit Alexa Fluor 568, anti-mouse Alexa Fluor 647 and anti-rabbit Alexa Fluor 633. All secondary antibodies were provided by Molecular Probes (Invitrogen) and used 1:1000 in PBS. DAPI was also used to stain for cell nuclei.

Both retinal flat mounts and sections were mounted with Vectashield (Vector Laboratories, 42 Burlingame, CA, USA) and imaged using either Leica laser SP5 or SP8 confocal microscopy systems.

### 2.8. Image Processing and Quantification

Images from both sections and whole retinal flat mounts were processed with the ImageJ software (US National Institutes of Health, Bethesda, Md., USA). Quantifications were based on analysis of at least three animals. We analyzed a minimum of two sections per mouse, and three random fields per section. For each flat mount, we imaged at least three random fields.

To quantify the number of $YFP^+$ cells differentiating into ganglion-amacrine neurons in flat mounts, $YFP^+$ total cells and double positive $YFP^+/CALR^+$ cells were counted in at least five random fields per animal (20× objective). The transdifferentiation rate was expressed as the percentage of $YFP^+/CALR^+$ cells over the total $YFP^+$ cells present in each field.

Similarly, the number of proliferating MGCs (Fig. 1d, S1d) was represented as the percentage of $phH3^+/YFP^+$ or $PCNA^+/YFP^+$ cells over the total $YFP^+$ cells counted in each imaged field.

$YFP^+$ and $YFP^+/Nestin^+$ cells were counted in at least five random fields from two different retinae per treatment group. The percentage of $Nestin^+$ cells was expressed with respect to the total $YFP^+$ MGCs counted in each field (Fig. S2d, e).

Quantification of the $YFP^+$ hybrids in retinal flat mounts of $R26/BM^{CRE\text{-}RFP}$ and GFAP-Cre/$BM^{R26Y}$ mice was evaluated by counting the $YFP^+$ cells in ten random fields per animal (20× objective). The percentage of $YFP^+$ hybrids was expressed with respect to either the total $RFP^+$ BMCs (Fig. 3e, f) or the $DAPI^+$ cells (Fig. S7e) present in each field.

### 2.9. Statistical Analysis

For statistical analysis, data were expressed as mean ± S.E.M. We used either unpaired, two-tailed Student's *t*-test, One-way or Two-way Anova (followed by Tukey's multiple comparisons test), as indicated in the figure legends. All statistical tests and graphs were generated using the Prism 7.0 software (GraphPad, San Diego, CA). A p value < 0.05 was considered significant (*, $p < 0.05$; **, $p < 0.01$; ***, $p < 0.001$; ****, $p < 0.0001$; ns, not significant).

## 3. Results

### 3.1. NMDA-damage Stimulates Müller Glia Cells (MGCs) Proliferation and Dedifferentiation

Intravitreal injection of NMDA was used to induce apoptosis of ganglion and amacrine neurons in a group of GFAP-Cre/R26Y mice, which carry glial cells genetically labeled in green (Fig. 1a).

We investigated the localization and the morphology of $YFP^+$ cells in retinal sections, 24 h (24 hpi) and 4 days (4 dpi) post-injury. As expected, we found that YFP expression co-localized with glutamine synthetase (GS), a known marker of glia cells that spans the entire thickness of the retinal tissue (Fig. 1b, yellow arrows). To further distinguish between MGCs and astrocytes, we performed staining for retinaldehyde-binding protein (CRALBP), which is specifically expressed in MGCs, but not in astrocytes. Staining was performed in retinal flat mounts, where expression of selected markers can be pinpointed to a specific retinal layer (Fig. S1a). We only found a few $YFP^+$-$CRALBP^-$ cells localized just below the ganglion cells layer; these cells were characterized by an astrocyte-like morphology (Fig. S1b bottom panels). However, within the retinal layers, the YFP signal co-localized with the MGC-specific marker CRALBP (Fig. S1b upper panels), meaning that the GFAP-Cre/R26YFP mouse model can be used to efficiently track MGCs.

We then FACS-sorted YFP-positive cells from either control (i.e., PBS-treated) or damaged (i.e., NMDA-treated) retinae at different times post-injection (Fig. S1c) to analyze gene expression patterns. Compared to those isolated from PBS-injected controls, $YFP^+$ cells sorted from NMDA-damaged retinae showed a tendency to up-regulate

numerous retinal progenitor genes 24 hpi, including *Pax6*, *Nestin*, *Chx10*, *Math3*, *Ascl1* and *Sox2* (Fig. 1c, left panel). Some of these trends were maintained 4 dpi (e.g. *Chx10*, *Ascl1*, *Sox2*), even though expression levels were found to slightly decrease (Fig. 1d, right panel). Expression of other genes, however, did not appear to be increased with respect to the PBS-injected control 4 dpi (e.g. *Pax6*, *Nestin*, *Math3*). Interestingly, *Cyclin D1* expression was strongly upregulated 24 hpi, and its levels remained high 4 dpi (Fig. S1d).

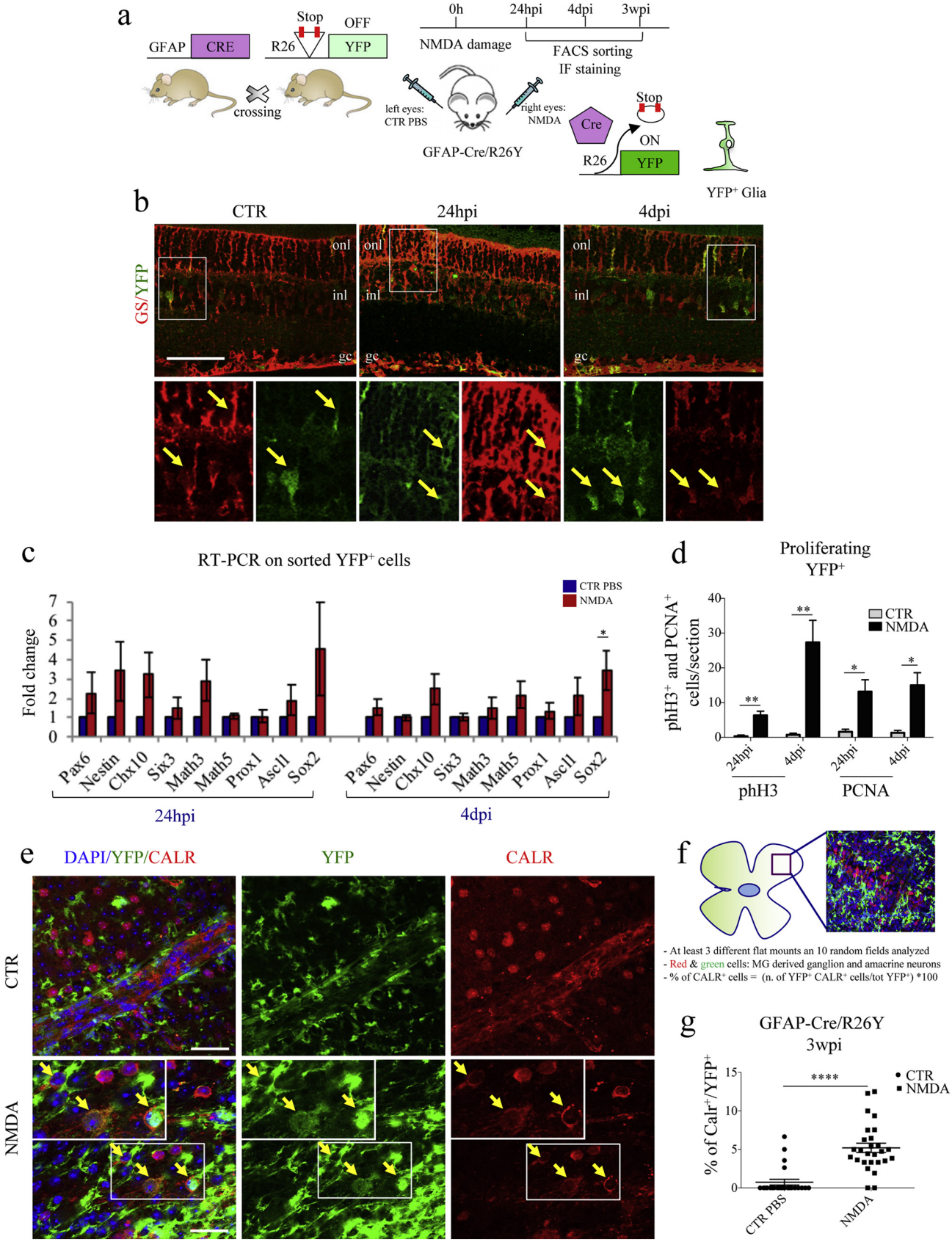

Since Cyclin D1 is expressed in the $G_1$ phase of the cell cycle and in proliferative cells (Kohno et al., 2006), our results suggested that MGCs could re-enter the cell cycle following NMDA damage. We validated these findings by staining both retinal sections (Fig. S1e) and flat mounts (Fig. S1f) for two well-known proliferation markers, namely proliferating cell nuclear antigen (PCNA) (Maga and Hubscher, 2003) and phosphorylated histone H3 (phH3) (Goto et al., 1999). In NMDA-damaged retinae, we found a number of $YFP^+$ cells that were also positive for PCNA and phH3, both at 24 hpi and 4 dpi (Figs. 1d, S1e, f). In the control samples, however, no $PCNA^+/YFP^+$ or $phH3^+/YFP^+$ cells were present (Figs. 1d, S1e, f). Overall, our data indicates that, following NMDA-damage, MGCs can re-enter the cell cycle and dedifferentiate, re-activating expression of neural and retinal progenitor genes.

To characterize the differentiation potential of $YFP^+$ cells, we followed their fate in the long term. In particular, we stained retinal flat mounts for calretinin (CALR), 3 weeks post-injection (3 wpi). CALR is a specific marker of ganglion and amacrine cells (Chiquet et al., 2005; Pasteels et al., 1990; Mojumder et al., 2008), which are the cell types that undergo apoptosis following NMDA-damage (Lucas and Newhouse, 1957; Siliprandi et al., 1992; Sucher et al., 1997). We found that, 3 wpi, 5% of the $YFP^+$ cells were also expressing CALR (Fig. 1e, f, g), suggesting that reprogrammed MGCs could re-differentiate towards a neuronal cell fate. We also qualitatively confirmed our data by finding that, 3 wpi, some $YFP^+$ cells were expressing beta-III tubulin (Fig. S1g), another ganglion cell-specific marker (Jiang et al., 2015).

### 3.2. Dedifferentiation of Müller Glia Cells is Affected by Perturbation of the SDF1/CXCR4 Signaling Axis

NMDA-damage was associated with an overall up-regulation of SDF1 expression, 24 hpi (Fig. 2a). Moreover, $YFP^+$ cells sorted from damaged GFAP-Cre/R26Y retinae were found to express SDF1 at higher levels than $YFP^+$ cells isolated from control samples (Fig. S2a). On the basis of these findings, we hypothesized that activation of the SDF1/CXCR4 pathway could be involved in the de-differentiation process of MGCs.

To investigate the validity of our hypothesis, we injected the SDF1 chemokine in a group of NMDA-damaged GFAP-Cre/R26Y mice (Fig. 2b; Group B). Another group of NMDA-treated mice was intraperitoneally injected with the SDF1 antagonist AMD3100 (Fig. 2b; Group C). An additional group only received NMDA-injection (Fig. 2b; Group A). We FACS-sorted $YFP^+$ cells 4 dpi from retinae belonging to each of these treatment groups (Fig. S2b), and we analyzed the expression of neural and retinal progenitor genes. We found that $YFP^+$ cells sorted from the SDF1-treated retinae showed a more de-differentiated, retinal progenitor-like phenotype (Fig. 2c). In particular, expression of *Pax6*, *Nestin*, *Six3*, *Math3*, *Math5*, and *Prox1* was increased. *Cyclin D1* expression was also strongly up-regulated (Fig. 2d). Expression of these genes was instead severely decreased in the $YFP^+$ cells sorted from retinae of mice that had received AMD3100 treatment (Fig. 2c, d).

Interestingly, SDF1 treatment was also associated with an increase in the total number of $YFP^+$ cells, as analyzed by FACS (Fig. S2c). Moreover, compared to NMDA-injected controls, the number of $YFP^+/Nestin^+$ cells 4 dpi was increased in SDF1–treated retinae, and reduced in AMD3100-treated ones (Fig. S2d, e). Overall, these results suggest that SDF1-treatment can increase the de-differentiation and the proliferation of MGCs.

Importantly, even the number of $YFP^+/CALR^+$ cells 3 wpi was significantly higher in retinal flat mounts harvested from SDF1-treated mice, as compared to NMDA-damaged controls (Fig. 2e, f). AMD3100-treatment, instead, was associated with a strong reduction in the number of $YFP^+/CALR^+$ cells (Fig. 2e, f). In other words, our results suggest that the number of MGC-derived ganglion and amacrine cells is increased by SDF1-treatment, and decreased by inhibition of the SDF1-CXCR4 axis.

To investigate whether newly generated $YFP^+/CALR^+$ cells would undergo apoptosis, we performed TUNEL staining on retinal flat mounts of GFAP-Cre/R26Y lineage tracing mice. As a control, we confirmed that the number of apoptotic $TUNEL^+$ cells was significantly higher in damaged retinae as compared to control ones, 1 week post-injection (1 wpi, Fig. S3a, c). The number of apoptotic cells was instead reduced 3 wpi (Fig. S3b, c), most likely because NMDA-dependent cell death had already largely been completed at this time point. Indeed, 3 wpi, very few $YFP^+/CALR^+$ cells were also $TUNEL^+$, in all treatment groups (Fig. S3d).

We also wondered whether NMDA-damage and SDF1 administration could cause infiltration of phagocytic cells, such as microglia and macrophages. We therefore evaluated the presence of MAC-1 expressing cells in total retinae of wild type mice using FACS analysis, 24 hpi and 4 dpi (Fig. S4a, b). We found a slight but not significant increase in the percentage of $MAC\text{-}1^+$ cells in the NMDA-damaged retinae harvested 24 hpi as compared to the PBS-injected controls (Fig. S4a, b). The percentage of infiltrated $MAC\text{-}1^+$ cells decreased drastically 4 dpi (Fig. S4a). SDF1 administration did not alter the percentage of $MAC\text{-}1^+$ macrophages (Fig. S4a, b). Furthermore, $CALR^+$ cells derived from $YFP^+$ cells were negative for the expression of MAC-1 3 wpi (Fig. S4c).

Collectively, our data suggest that, following NMDA-damage, MGCs can undergo dedifferentiation and re-enter the cell cycle. They can then re-differentiate into $CALR^+$ cells, without undergoing apoptosis. These events are regulated by the SDF1-CXCR4 signaling axis, at least partially.

### 3.3. The SDF1/CXCR4 Axis Regulates Recruitment of Endogenous Bone Marrow Cells (BMCs), Which can Then Fuse With Retinal Cells

As MGC de-differentiation is regulated by the SDF1/CXCR4 signaling axis, which also induces mobilization of endogenous BMCs, we

**Fig. 1.** Müller glial cells (MGCs) undergo reprogramming and differentiate into $CALR^+$ cells following NMDA-damage. (a) Experimental scheme. We used transgenic GFAP-Cre/R26Y mice. In these mice, ubiquitous expression of YFP is impeded by the presence of a floxed-STOP codon, which can be excised by Cre recombinase. Expression of Cre recombinase is driven by the glial-specific GFAP promoter. As a consequence, the YFP reporter allows to trace glial cells. We injected NMDA in the right eyes to induce retinal degeneration. Left eyes were injected with PBS, as controls. We characterized $YFP^+$ cells at various time-points post-injection. (b) Representative immunostaining of retinal sections harvested from GFAP-Cre/R26Y mice sacrificed 24 hpi and 4 dpi. Higher magnification images (from the areas enclosed by the white boxes) are shown in the bottom panel. $YFP^+$ cells (green) are also positive for GS (red), a well-known glial marker (onl, outer nuclear layer; inl, inner nuclear layer; gc, ganglion cells layer). Scale bar: 100 μm. (c) RT-PCR expression analysis of neural stem cell and retinal progenitor genes using total RNA harvested from FACS-sorted $YFP^+$ cells of either PBS-treated (CTR) or NMDA-damaged (NMDA) retinae of GFAP-Cre/R26Y mice, 24 hpi and 4 dpi. Transcript levels are expressed as fold-changes relative to $YFP^+$ cells sorted from PBS-injected retinae. Data are represented as mean ± S.E.M. (n = 4). Statistical analysis is based on unpaired Student's *t*-test (24 hpi: Pax6, $p = 0.3533^{ns}$;Nestin, $p = 0.1704^{ns}$; Chx10, $p = 0.1009^{ns}$; Six3, $p = 0.3896^{ns}$; Math3, $p = 0.1157^{ns}$; Math5, $p = 0.5200^{ns}$; Prox1, $p = 0.8599^{ns}$; Ascl1, $p = 0.3695^{ns}$; Sox2, $p = 0.2774^{ns}$; 4 dpi: Pax6, $p = 0.2357^{ns}$; Nestin, $p = 0.3592^{ns}$; Chx10, $p = 0.0771^{ns}$; Six3, $p = 0.8952^{ns}$; Math3, $p = 0.4317^{ns}$; Math5, $p = 0.1218^{ns}$; Prox1, $p = 0.3917^{ns}$; Ascl1, $p = 0.2790^{ns}$; Sox2, $p = 0.0378^{*}$). (d) Quantification of proliferating MGCs. Results are presented as number of counted $PCNA^+/YFP^+$ and $phH3^+/YFP^+$ cells per section, 24 hpi and 4 dpi, both for PBS-treated (CTR) and NMDA-damaged (NMDA) retinae. Data are represented as mean ± S.E.M. (n = 3). Statistical analysis is based on unpaired Student's *t*-test (phH3: 24 hpi, $p = 0.0086^{**}$; 4 dpi, $p = 0.0042^{**}$; PCNA: 24 hpi, $p = 0.0103^{*}$; 4 dpi, $p = 0.0203^{*}$). (e) Immunostaining of retinal flat mounts from GFAP-Cre/R26Y mice sacrificed 3 weeks post-injection. Representative fields from PBS-injected (CTR) and NMDA-damaged (NMDA) retinae. $YFP^+$ cells (green) differentiating into $CALR^+$ cells (red) are indicated by yellow arrows. Nuclei were counterstained with DAPI (blue). Scale bar: 20 μm. (f) Schematic representation of the method used for counting marker-positive cells in retinal flat mounts. GFAP-Cre/R26Y mice were used for these experiments. $YFP^+$ and $YFP^+/CALR^+$ cells were counted in 10 random fields from at least three different retinal flat mounts for each treatment group. (g) Percentages of $YFP^+$ cells expressing CALR, 3 wpi. Cells were counted in 6–10 random fields for each flat mount harvested from either PBS-injected (CTR) and damaged (NMDA) retinae. Data are represented as mean ± S.E.M. (n = 3). Statistical analysis is based on unpaired Student's *t*-test ($p < 0.0001^{****}$).

evaluated whether mobilized BMCs could fuse with retinal MGCs. To test this hypothesis, we used chimeric R26Y/BM$^{CRE-RFP}$ mice, which carry BMCs expressing CRE and RFP. In this model, BMCs can be tracked by looking at RFP expression, whereas fusion events involving mobilized BMCs can be tracked by looking at simultaneous expression of RFP and YFP (Fig. 3a).

Firstly, we investigated the extent of BMC recruitment using FACS analysis. We injected a group of chimeric R26Y/BM$^{CRE-RFP}$ mice with either PBS or NMDA. We found NMDA-damage to be associated with enhanced recruitment of RFP$^+$ BMCs, which come to represent 4% of the total retinal cells 24 hpi (Fig. 3b, Fig. S5a). The amount of RFP$^+$ BMCs in damaged retinae decreased 4 dpi (Fig. 3b, Fig. S5a).

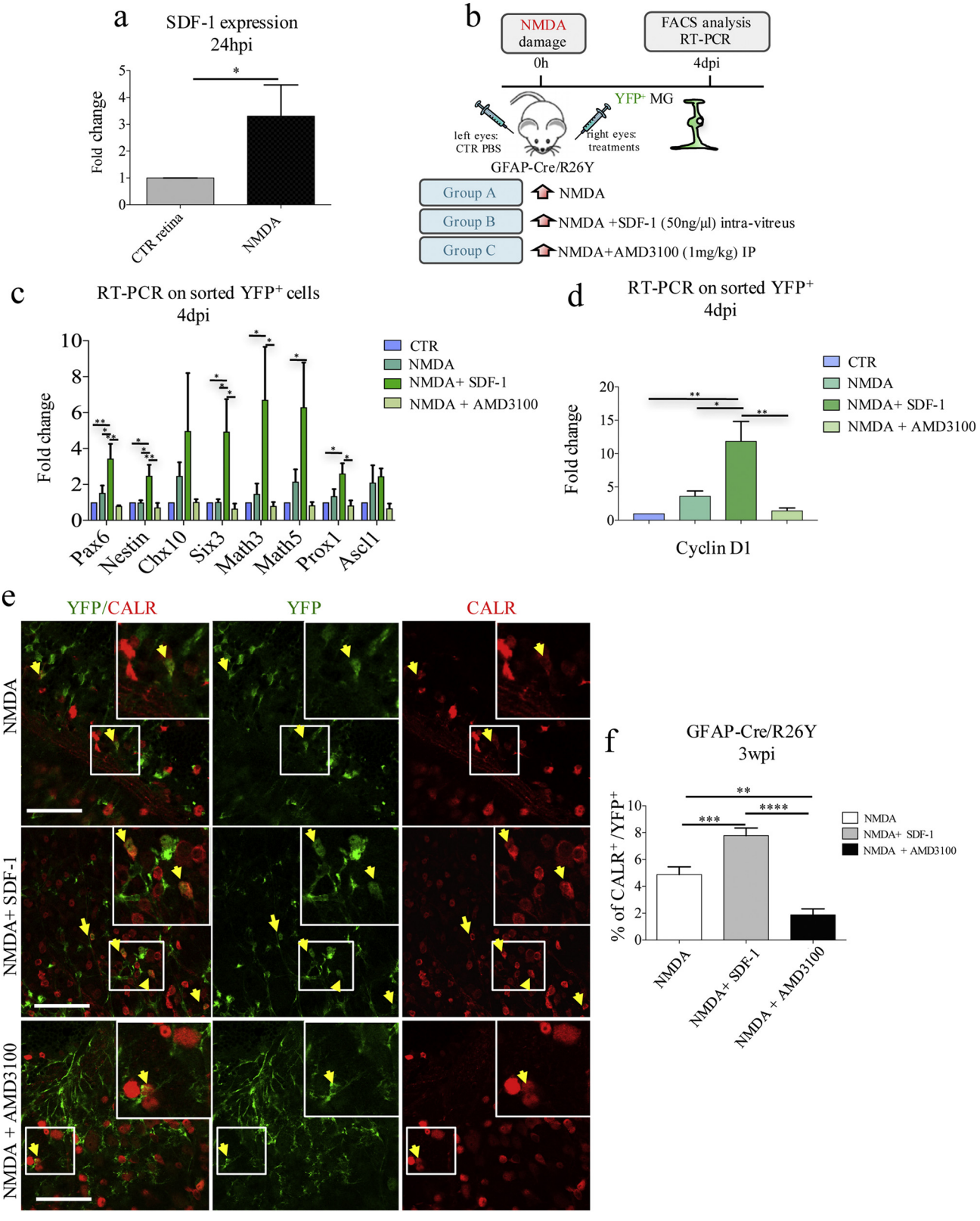

Secondly, we explored the effects of SDF1/CXCR4 axis modulation on damage-dependent BMC recruitment. We performed FACS analysis on retinal samples from R26Y/BM$^{CRE-RFP}$ mice that had been previously injected with NMDA, NMDA + SDF1 or NMDA + AMD3100 (Fig. 3a). As expected, the percentage of RFP$^+$ BMCs was significantly higher in the eyes that had received SDF1-treatment as compared to the ones that only received an NMDA injection, 24 hpi (Figs. 3c, S5b). In contrast, the percentage of RFP$^+$ BMCs was decreased in the group of mice that had been treated with AMD3100 (Figs. 3c, S5b).

Overall, our findings indicate that endogenous BMCs can be efficiently mobilized in response to tissue injury in <24 h, and that their migration is regulated by the SDF1-CXCR4 signaling axis.

Next, we evaluated fusion events. FACS analysis of retinae harvested from R26Y/BM$^{CRE-RFP}$ chimeric mice revealed that, after 24 h from NMDA-damage, approximately 3% of recruited RFP$^+$ BMCs were also expressing YFP, which we interpreted as bona fide hybrids derived from fusion events (Figs. 3d, S5c). These findings were also confirmed in retinal flat mounts (Fig. 3e, f). Interestingly, the percentage of RFP$^+$/YFP$^+$ hybrids further increased to 5.2% 4 dpi (Figs. 3d, S5c).

When compared to the total number of retinal cells, however, the number of YFP$^+$/RFP$^+$ hybrids was extremely low, suggesting that cell fusion with endogenous BMCs only occurred with low frequency. Nonetheless, we probably underestimated the number of hybrids formed in vivo due to BM chimerism. In fact, 6 weeks after BM replacement, only about 45% of BMCs were found to be RFP$^+$ (Fig. S5d, e).

Collectively, our data indicate that endogenous BMCs can be recruited through the activity of the SDF1/CXCR4 signaling axis and can fuse with resident retinal cells.

### 3.4. Mobilized Bone Marrow Cells Preferentially Fuse With Müller Glia Cells

To identify the retinal cell types capable of fusing with BMCs, we performed immunofluorescence staining for several markers, both in retinal flat mounts and in retinal sections of chimeric R26Y/BM$^{CRE-RFP}$ mice. In NMDA-damaged retinae, 24 hpi, we found that several RFP$^+$/YFP$^+$ hybrids were also expressing GS (Fig. 4a, b). This indicated that endogenous BMCs could fuse with glial cells of the retina. Importantly, the large majority of YFP$^+$/RFP$^+$ hybrids were also found to express CRALBP (Fig. S6a, b), indicating that fusion mainly occurs with MGCs, and not with astrocytes. Furthermore, we stained for bipolar (PKC), horizontal (calbindin, CALB), and photoreceptor (recoverin, REC) markers, but we could not observe any co-localization of these neuronal markers with YFP. However, we found some CALR$^+$ hybrids, suggesting that ganglion and amacrine neurons could also act as fusion partners (Fig. S6c).

To better characterize the frequencies of fusion events involving MGCs and ganglion/amacrine neurons, we generated two different types of chimeric mice, namely GFAP-Cre/BM$^{R26Y}$ (Fig. 4c) and Calr-Cre/R26Y/BM$^{RFP}$ (Fig. S6d). In the former, BMCs-MGCs fusion could be tracked by looking at YFP expression. In the latter, instead, co-localization of YFP and RFP was indicative of fusion between BMCs and ganglion/amacrine neurons. We found that 0.6% of the total retinal cells were positive for YFP expression in NMDA-damaged GFAP-Cre/BM$^{R26Y}$ eyes (Fig. 4d, e). However, only 0.7% of the RFP$^+$ BMCs recruited into damaged Calr-Cre/R26Y/BM$^{RFP}$ retinae were found to express YFP. This corresponded to the 0.03% of the total retinal cells (Fig. S6e–g). Therefore, we could conclude that fusion events involving ganglion/amacrine neurons were extremely rare, and that BMCs preferentially fused with MGCs.

### 3.5. BMC–MGC Hybrids Undergo Reprogramming to Then Differentiate Into Ganglion and Amacrine Cells

As the majority of fusion events occurred between BMCs and MGCs, we decided to follow up our study using chimeric GFAP-Cre/BM$^{R26Y}$ mice.

Firstly, we confirmed that YFP$^+$ hybrids generated following NMDA-damage expressed CRALBP (Fig. S7a, b). We also found that some of the YFP$^+$ hybrids were positive for MAC-1 24 hpi (Fig. S7c). However, we found that only 0.13% of the total Dapi$^+$ cells were TUNEL$^+$/YFP$^+$ hybrids in the NMDA-damaged retinae (Fig. S7d, e). In other words, only 24% of the total YFP$^+$ were found to be apoptotic. This suggested that BMCs largely fused with non-apoptotic MGCs and/or that the majority of the hybrids did not undergo apoptosis 24 hpi. Of note, very few hybrids were present in the control samples (0.02%) and none of them was found to be TUNEL$^+$ (Fig. S7d, e).

Secondly, to investigate the proliferative potential of these hybrids, we stained retinal sections for phH3. We found that, 24 hpi, many YFP$^+$ hybrids were positive for phH3 (Fig. S7f). Accordingly, YFP$^+$ hybrids sorted 24 hpi showed increased levels of the cell-cycle gene *cyclin D1*, as compared to the pull of total retinal cells (Fig. 5a).

Thirdly, to determine whether these hybrids were associated with a dedifferentiation phenotype, we also looked at expression of various pluripotency genes and retinal progenitor markers. With respect to YFP$^-$ retinal cells, hybrids were found to significantly up-regulate *Sox2*, *Pax6*, *Math3* and *CyclinD1* (Fig. 5a). We also observed a tendency for up-regulation of other retinal progenitor genes (i.e. *Nestin*, *Ascl1*, *Six3*, *Prox1*, and *Chx10*) and pluripotency markers (*Oct4* and *SSEA1*), but such increases were not statistically significant (Fig. 5a).

Lastly, we assessed whether MGCs-derived hybrids could ultimately differentiate into retinal neurons. Due to the nature of the induced damage, we focused on hybrids conversion into ganglion and amacrine neurons, using GFAP-Cre/BM$^{R26Y}$ chimeric mice. As a control, we excluded that irradiation and BM replacement could significantly alter the number of these neurons. More specifically, we compared the number of ganglion/amacrine cells in retinae of wild type mice with that of irradiated and transplanted animals. The absolute numbers of CALR$^+$ neurons were comparable in both groups, and, therefore, unaffected by the irradiation and transplantation procedures (Fig. S8a). Approximately 15% of the YFP$^+$ cells were expressing CALR 3 wpi (Fig. 5b, c, Fig. S8b, yellow arrows), suggesting that MGC-derived hybrids could differentiate towards a neuronal fate following NMDA-damage. However, many of

**Fig. 2.** Modulation of the SDF1/CXCR4 axis affects Müller glial cell reprogramming and their differentiation into CALR$^+$ cells. (a) RT-PCR analysis of SDF1 expression using RNAs extracted from PBS-treated (CTR) and NMDA-damaged (NMDA) retinae, 24 hpi. Transcript levels are expressed as fold-changes relative to CTR retinae. Data are represented as mean ± S.E.M. (n = 3). Statistical analysis is based on unpaired Student's *t*-test ($p = 0.0372^{*}$). (b) Experimental scheme: GFAP-Cre/R26Y lineage tracing mice were randomly divided into three treatment groups: NMDA-damage (group A); NMDA-damage followed by SDF1-treatment (group B); NMDA-damage followed by AMD3100-treatment (group C). Mice were sacrificed 4 dpi to investigate changes in the dedifferentiation and reprogramming state of YFP$^+$ cells, using FACS and RT-PCR analysis. (c, d) RT-PCR analysis of retinal progenitors (c) and cell-cycle (d) gene expression in YFP$^+$ cells FACS-sorted 4 dpi from GFAP-Cre/R26Y mice belonging to the four treatment groups (CTR, NMDA, NMDA+SDF-1, NMDA+AMD3100). Transcript levels are expressed as fold-changes relative to YFP$^+$ cells sorted from PBS-injected retinae. Data are represented as mean ± S.E.M. (n ≥ 5). Statistical analysis is based on One-way Anova (Pax6, $p = 0.0023^{**}$; Nestin, $p = 0.0052^{**}$; Chx10, $p = 0.2315^{ns}$; Six3, $p = 0.0081^{**}$; Math3, $p = 0.0233^{*}$; Math5, $p = 0.0393^{*}$; Prox1, $p = 0.0189^{*}$; Ascl1, $p = 0.3125^{ns}$; cyclinD1, $p = 0.0015^{**}$), followed by Tukey's multiple comparisons test (significance indicated in the figure). (e) Representative immunostaining images from retinal flat mounts harvested 3 wpi from GFAP-Cre/R26Y lineage tracing mice belonging to the four treatment groups (NMDA, NMDA+SDF-1, NMDA+AMD3100). Co-localization between YFP (green) and CALR (red) is indicated by yellow arrows. Cell nuclei were counterstained with DAPI (blue). Representative higher magnification images are shown in the white boxes. Images were taken from 10 random fields for each retinal flat mount, from at least three different mice per treatment group (n = 3). Scale bar: 40 μm. (f) Percentages of YFP$^+$/CALR$^+$ double positive cells with respect to total YFP$^+$ cells in retinal flat mounts of GFAP-Cre/R26Y lineage tracing mice belonging to the different treatment groups (NMDA, NMDA+SDF-1, NMDA+AMD3100), sacrificed 3 wpi. YFP and CALR immunopositive cells were counted in random fields (20× objective) from three independent experiments (n = 3, NMDA, fields = 30; NMDA+SDF-1, fields = 43; NMDA+AMD3100, fields = 21). Statistical analysis is based on One-way Anova ($p < 0.0001^{****}$) followed by Tukey's multiple comparisons test (significance indicated in the figure).

the hybrids were still positive for GS expression, indicating that they retained their glia identity (Fig. S8b, magenta arrows). Additionally, a percentage of YFP$^+$/GS$^+$ cells was also expressing CALR (Fig. S8b, red arrows), suggesting that, 3 wpi, hybrids could be found in an intermediate differentiation stage. Of note, none of the hybrids were expressing MAC-1 3 wpi (Fig. S8c).

Collectively, our data indicate that, following damage-induced recruitment of BMCs, MGCs can undergo fusion-mediated

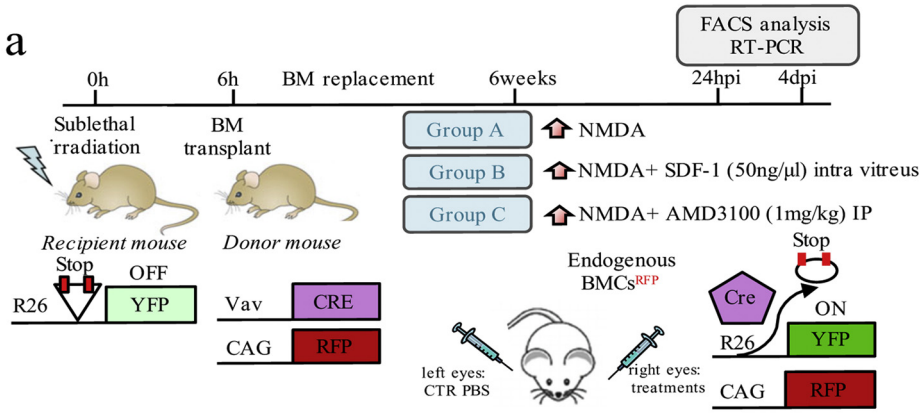


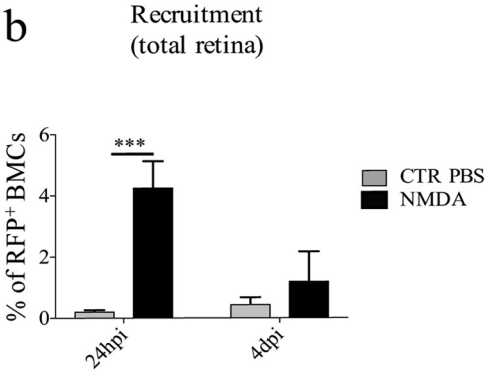


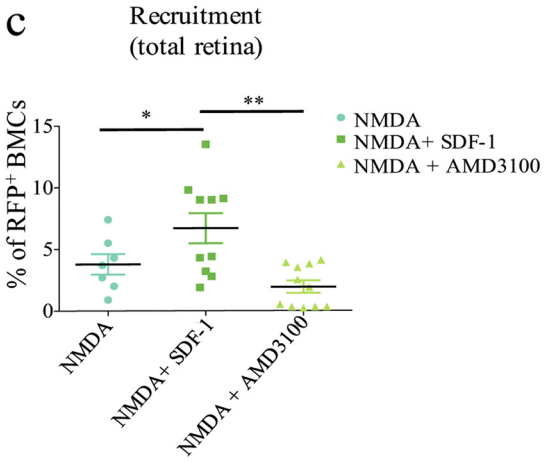


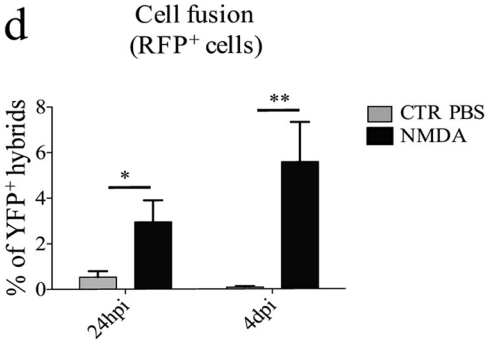


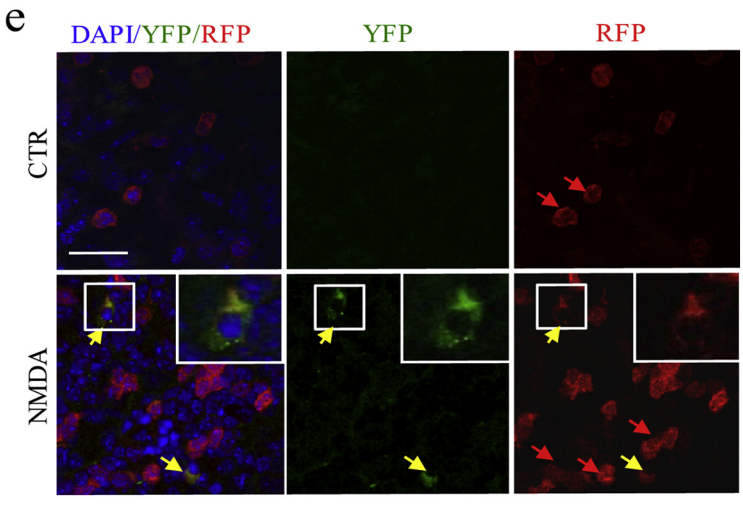


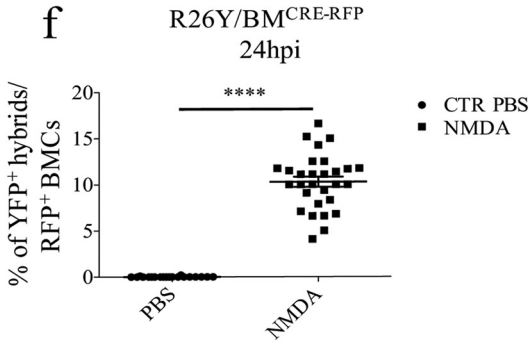

reprogramming. Importantly, reprogrammed BMC-MGC hybrids can differentiate towards a neuronal fate, expressing markers of ganglion and amacrine cells.

## 4. Discussion

In this study, we have shown that NMDA-induced mobilization of BMCs into the retina is associated with fusion events that stimulate MGC proliferation and dedifferentiation. Newly generated hybrids can give rise to $CALR^+$ cells three weeks post-injury. All of these events are affected by modulation of the SDF1/CXCR4 signaling axis.

Damage-induced up-regulation of SDF1 is not unexpected, as increased SDF1 expression has been extensively correlated with tissue injury and hypoxia (Lima E Silva et al., 2007; DeLeve et al., 2016; Mocco et al., 2014; Yu et al., 2010), even in retinal models of ischemia (Lai et al., 2008) and RPE damage (Li et al., 2006). Similarly, the SDF1/CXCR4 axis is well known to play a major role in BMC mobilization (Cheng and Qin, 2012; Nervi et al., 2006; Hattori et al., 2001; Lima E Silva et al., 2007). Indeed, intravitreal administration of SDF1 has already been shown to enhance BMC recruitment in a model of sodium iodate-induced retinal degeneration (Enzmann et al., 2017).

Our study further elucidates the possible mechanisms underlying BMC-dependent regeneration in the retina, investigating the role and contribution of cell fusion events. In fact, fusion of BMCs with resident cells has already been implicated in the repair of several tissues and organs, including heart (Nygren et al., 2004), liver (Petersen et al., 1999; Lagasse et al., 2000; Pedone et al., 2017), gut (Rizvi et al., 2006), skeletal muscle (Ferrari et al., 1998) and central nervous system (Johansson et al., 2008; Altarche-Xifro et al., 2016; Sanges et al., 2013, 2016).

We have shown that NMDA-damage and cell fusion are associated with MGC spontaneous re-entry into the cell cycle and re-activation of multiple retinal progenitor genes. Our observations are consistent with numerous studies that have revealed how MGCs and retinal progenitor cells are similar with respect to gene expression patterns (Blackshaw et al., 2004; Livesey et al., 2004). This is not particularly surprising, as MGCs are derived from multipotent progenitor cells (Young, 1985; Turner and Cepko, 1987). Astrocytes, instead, have a different developmental origin, and migrate into the retina through the optic nerve after being generated in the brain (Stone and Dreher, 1987; Watanabe and Raff, 1988). Consequently, MGCs are more similar to progenitor cells than retinal neurons or astrocytes are, and they somehow retain the potential to reacquire their progenitor state under certain circumstances (Jadhav et al., 2009; Blackshaw et al., 2004). For instance, rodent MGCs can dedifferentiate and re-enter the cell cycle following cytotoxicity induced by intravitreal administration of various chemicals, including ouabain and NMDA (Sahel et al., 1990; Ooto et al., 2004; Karl et al., 2008; Todd et al., 2015). Similarly, they can start proliferating following MNU-mediated damage of the photoreceptors layer (Wan et al., 2008).

The frequency of such events, however, is extremely low, and the endogenous neurogenic potential of mammalian MGCs is not sufficient for the rescue of retinal functionality (Karl and Reh, 2010). Nonetheless, various studies have shown that MGC dedifferentiation can be promoted in a number of ways, that include, for instance, treatment with mitogenic factors, such as insulin, EGF and Wnt3a (Close et al., 2006; Karl et al., 2008; Takeda et al., 2008; Osakada et al., 2007; Todd et al., 2015; Ringuette et al., 2016). In this study, we decided to use the SDF1 chemokine. Alternatively, the neurogenic state of MGCs can also be induced by over-expression of specific transcription factors, such as *Ascl1* (Ueki et al., 2015; Pollak et al., 2013). *Ascl1* is of particular interest because it has been extensively described as a key player in the MGC-mediated retinal regeneration in early vertebrates, but it is not spontaneously upregulated in mammalian MGCs after injury (Goldman, 2014). Remarkably, MGC reprogramming ability can be further increased when *Ascl1* over-expression is combined with inhibition of a histone deacetylase, which results in a more open chromatin state that favors accessibility at key gene loci (Jorstad et al., 2017).

In this context, MGC-derived neurons were reported to be mainly generated through direct transdifferentiation, unless combined with EGF-treatment (Jorstad et al., 2017). In our study, instead, we detected a dedifferentiation-associated proliferative phase, followed by re-differentiation. We believe that our results complement the ones from Jordstad and colleagues. In fact, transdifferentiation and cell fusion could both be mechanisms contributing to tissue regeneration, and there is no conclusive evidence showing that they are mutually exclusive. They could occur independently from each other under different conditions or, alternatively, they could act simultaneously and, possibly, synergistically. In accordance with our hypothesis, it has been shown that, following retinal damage, adult murine MGCs can contribute to neuronal regeneration by passing through a proliferative stage (Karl et al., 2008; Ooto et al., 2004; Todd et al., 2015; Webster et al., 2017). Interestingly, this re-entry into the cell cycle was found to be mediated by cyclin D1-related pathways, which is also consistent with our findings (Osakada et al., 2007; Ooto et al., 2004). Additionally, it is important to specify that we decided to focus on cell fusion, without using any of the genetic manipulations or chemical inhibition that are now known to enhance transdifferentiation. However, we cannot fully exclude that some of the cell identity changes we reported could be due to transdifferentiation events.

In accordance with published literature (Alvarez-Dolado et al., 2003; Weimann et al., 2003a, 2003b), we found that fusion events occur with an extremely low frequency. In this direction, it is interesting to note that fusion frequency can significantly increase following injury, degeneration or chronic inflammation of the central nervous system (Johansson et al., 2008; Sanges et al., 2013). This could be explained by the fact that neuropathology is associated with an enhancement of the chemokine-mediated recruitment and engraftment of BMCs,

**Fig. 3.** Endogenous bone-marrow cells migrate into NMDA-damaged retinae and fuse with resident retinal cells. (a) Schematic representation of the experimental plan. We used chimeric $R26Y/BM^{CRE\text{-}RFP}$ mice, generated by replacing the BM of R26Y mice with the BM of CAG-RFP/Vav-Cre donor mice. In R26Y mice, ubiquitous expression of YFP is impeded by the presence of a floxed-STOP codon, which can be excised by Cre recombinase. BMCs from CAG-RFP/Vav-Cre mice express both RFP and Cre recombinase: RFP expression is driven by a ubiquitous CAG promoter, whereas Cre recombinase is under the control of the hematopoietic-specific Vav promoter. As a result, following BM replacement, cell fusion events between BMCs ($Cre^+/RFP^+$) and retinal cells (R26Y) can be tracked by looking at YFP expression. Six weeks after BM replacement, we intravitreally injected the right eyes of $R26Y/BM^{CRE\text{-}RFP}$ mice randomly divided into three treatment groups: NMDA-damage (group A); NMDA-damage followed by SDF1-treatment (group B); NMDA-damage followed by AMD3100-treatment (group C). Left eyes were injected with PBS as a control. Mice were sacrificed 24 hpi and 4 dpi for RT-PCR and FACS analysis. (b) Percentages of recruited $RFP^+$ BMCs with respect to total retinal cells of PBS- and NMDA-injected chimeric $R26Y/BM^{CRE\text{-}RFP}$ mice, as analyzed by FACS 24 hpi and 4 dpi. Data are represented as mean ± S.E.M. (24 hpi, n = 8; 4 dpi: n = 4). Statistical analysis is based on unpaired Student's *t*-test (24 hpi, $p = 0.0004^{***}$; 4 dpi, $p = 0.4244^{ns}$). (c) Percentages of recruited $RFP^+$ BMCs with respect to total retinal cells of $R26Y/BM^{CRE\text{-}RFP}$ chimeric mice belonging to the various treatment groups (NMDA, NMDA + SDF1, NMDA + AMD3100), as analyzed by FACS. Data are represented as mean ± S.E.M. (NMDA, n = 8; NMDA+SDF-1, n = 10; NMDA+AMD3100, n = 10). Statistical analysis is based on One-way Anova ($p = 0.0023^{**}$) followed by Tukey's multiple comparisons test (significance indicated in the figure). (d) Percentages of $YFP^+$ hybrids in PBS- and NMDA-treated retinae of $R26Y/BM^{CRE\text{-}RFP}$ chimeric mice, with respect to total recruited $RFP^+$ BMCs, 24 hpi and 4 dpi. Values represent means ± S.E.M. (24 hpi: CTR, n = 13 and NMDA, n = 8; 4 dpi: CTR, n = 4 and NMDA, n = 4). Statistical analysis is based on unpaired Student's *t*-test (24 hpi, $p = 0.0105^{*}$; 4 dpi, $p = 0.0083^{**}$). (e) Representative immunostaining of PBS- (CTR) and NMDA-injected retinal flat mounts of chimeric $R26Y/BM^{CRE\text{-}RFP}$ mice, harvested 24 hpi (n = 3). Recruited $RFP^+$ BMCs are indicated by red arrows, whereas $RFP^+/YFP^+$ hybrids are indicated by yellow arrows. Cell nuclei were counterstained with DAPI (blue). Zoomed images of representative areas included in the white boxes are shown in the upper-right corners. Scale bar: 40 μm. (f) Percentage of $RFP^+/YFP^+$ hybrids with respect to total $RFP^+$ BMCs in PBS- and NMDA-injected retinae of chimeric $R26Y/BM^{CRE\text{-}RFP}$ mice sacrificed 24 hpi. We counted cells in 7–10 random fields for each retinal flat mount (n = 3). Statistical analysis is based on unpaired Student's *t*-test ($p < 0.0001^{****}$).

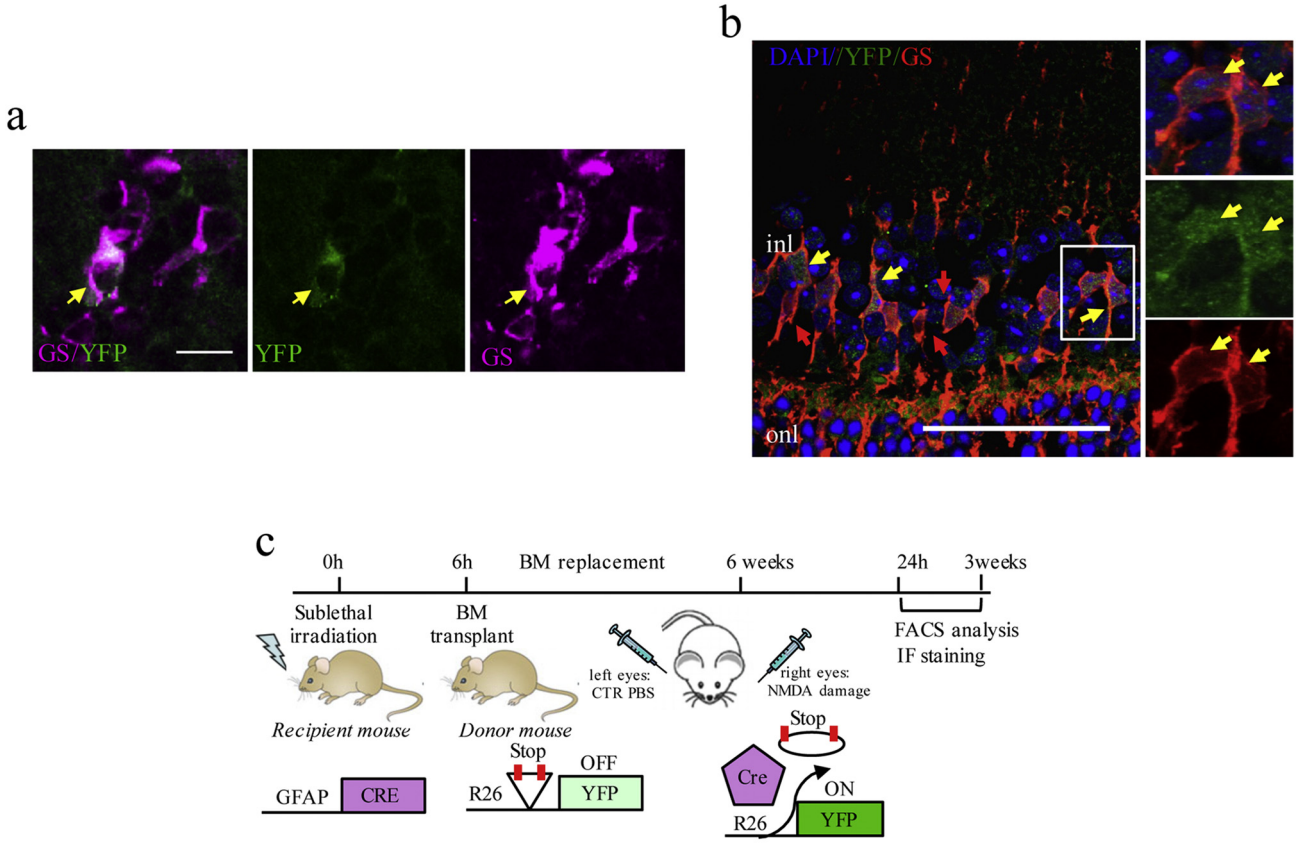
a
GS/YFP
YFP
GS
b
DAPI//YFP/GS
inl
onl
c
0h
6h
BM replacement
6 weeks
24h
3weeks
Sublethal irradiation
BM transplant
left eyes: CTR PBS
right eyes: NMDA damage
FACS analysis
IF staining
Recipient mouse
Donor mouse
Stop
OFF
GFAP
CRE
R26
YFP
Stop
Cre
ON
R26
YFP
d
GFAP-Cre/R26Y
24hpi
% of YFP+ hybrids
1.5
1.0
0.5
0.0
CTR PBS
NMDA
CTR PBS
NMDA
e
CTR
NMDA
DAPI/YFP/GS
inl
onl
YFP
GS

especially around the injury site (Priller et al., 2001). Accordingly, we found that retinal damage is essential for hybrid formation in vivo, and that fusion frequency can be enhanced via modulation of the SDF1/CXCR4 signaling axis.

Although we did not investigate the exact nature of the recruited BMCs, we observed that some hybrids were positive for MAC-1 in the short term. This could indicate that hybrids are phagocytized by macrophages in the short term. Nonetheless, we also found plenty of MAC-1-negative hybrids, suggesting that fusion with other BM sub-populations occurs. In support of this hypothesis, we found that SDF1 treatment does not significantly alter macrophage infiltration. In other words, the increase in fusion frequency associated with SDF1 administration does not correlate with an increase in the number of macrophages. Similar findings were reported by Enzmann and colleagues, who actually showed that SDF1 increases migration of Sca-1+ primitive hematopoietic cells (Enzmann et al., 2017).

Importantly, in the long-term, none of hybrids were expressing MAC-1, suggesting that they were not cleared from the tissue. Moreover, the majority of BMC-MGC hybrids were not apoptotic in the short term and they were able to survive within the retinal tissues. This was indicated by the fact that their number increased from 24 hpi to 4 dpi, while the amount of total BMCs recruited into the retina decreased.

Our finding that BMC-MGC hybrids can then re-differentiate towards a neuronal fate is also consistent with numerous published studies that show how MGCs can convert into retinal neurons upon injury (Wan et al., 2008; Ooto et al., 2004; Karl et al., 2008). Indeed, generally speaking, glial cells of the central nervous system can be induced towards a neuronal fate (Heins et al., 2002; Berninger et al., 2007; Heinrich et al., 2011, 2014; Karow et al., 2012; Guo et al., 2014; Su et al., 2014; Niu et al., 2013).

In many cases, however, we observed that cell fate conversion was not complete, at least 3 weeks post-injury: many hybrids were found to express only GS, while others were found in an intermediate differentiation stage, expressing both glial and neuronal markers. More time could be needed in order for hybrid-derived neurons to acquire a mature phenotype; alternatively, they could be unable to fully differentiate. Indeed, glia-derived new neurons in the CNS generally fail to mature on their own (Niu et al., 2013; Su et al., 2014). Nonetheless, they can be induced to acquire a more complete neuronal phenotype by various treatments, including exposure to BDNF, noggin and BMP (Niu et al., 2013, Su et al., 2014). Similarly, the maturity of MGC-derived neurons could potentially be controlled by extrinsic and/or intrinsic factors. Accordingly, the specific fate of MGC-derived neurons can be regulated via administration of specific factors [e.g. RA, promoting generation of bipolar cells (Ooto et al., 2004)] or via over-expression of defined genes [e.g. *Math3-NeuroD* or *Crx-NeuroD*, promoting formation of amacrine cells and photoreceptors respectively (Ooto et al., 2004), or *Atoh7*, stimulating differentiation into retinal ganglion cells (Song et al., 2015)]. This could be of valuable importance to ensure generation of the exact neuronal type that has been injured or lost.

Finally, it is important to stress that we mainly focused on hybrid conversion into ganglion and amacrine neurons, since activated MGCs tend to differentiate into the cell type that has been damaged (Wan et al., 2008; Sanges et al., 2013, 2016). However, we cannot fully exclude that reprogrammed MGCs could generate other retinal cell types.

Unfortunately, electroretinogram (ERG) tests did not allow us to satisfactorily evaluate the extent to which hybrid-derived neurons could contribute to functional recovery. This is most likely due to the fact that the frequency of fusion events and the number of newly generated neurons are currently too low to affect global retinal function. Functional conversion of hybrid-derived cells could probably be confirmed via patch clamp recording of individual neurons. In our opinion, however, a therapeutic readout could possibly be achieved only in the future, after optimization of multiple aspects, including: BMC mobilization, fusion efficiency, hybrids reprogramming and acquisition of a fully mature neuronal phenotype. As an example, we exclusively mobilized BMCs by local administration of SDF1 in the eye. Such treatment is probably less efficient than the use of other mobilizing agents at the systemic level. The use of G-CSF, for instance, could improve the efficiency of BMC recruitment into the damaged retina and lead to enhanced functional rescue, especially if coupled with local SDF1 administration. Indeed, coupling SDF1 intravitreal administration with systemic mobilization has been shown to result in significantly enhanced BMC recruitment into damaged retinae (Enzmann et al., 2017).

In conclusion, we have shown that cell fusion is one of the mechanisms underlying MGC plasticity in the adult mammalian retina. MGC ability to dedifferentiate and proliferate is dependent on the recruitment of their fusion partners, endogenous BMCs. Migration of BMCs is, in turn, regulated by the SDF1/CXCR4 signaling axis. As a result, modulation of the SDF1/CXCR4 pathway can affect MGC plasticity, and the extent to which MGCs can contribute to the endogenous regeneration of damaged retinal tissue.

Compared to cell therapy approaches, strategies aiming at the enhancement of endogenous regeneration would offer a number of significant advantages. In fact, despite being promising for the treatment of retina-related conditions, cell therapy can raise controversial concerns with respect to the risk of tumorigenesis (Tucker et al., 2011). Additionally, it is associated with problems regarding the correct integration of the transplanted cells within the host tissue. Approaches focusing on the enhancement of endogenous regenerative capacities could overcome many of these limitations. As an example, new neurons would be autologous by definition, and they would be generated directly in the vicinity of the injury, where they are needed.

Undoubtedly, we still are in the very early stages of therapies based on the endogenous regeneration. In this perspective, our study represents an important proof-of-principle that such therapeutic strategies could be possible in mammals.

## Funding Sources

This work was supported by an ERC grant (242630-RERE, to M.P.C.), the Ministerio de Economia y Competitividad and FEDER funds (SAF2011-28580, BFU2014-54717-P, and BFU2015-71984-ERC to M.P.C.), an AGAUR grant from Secretaria d'Universitats i Investigacio´ del Departament d'Economia I Coneixement de la Generalitat de Catalunya (2014SGR1137 to M.P.C.), Velux Stiftung (976 to M.P.C.), Ferrer International (to M.P.C., D.S.) Juan de la Cierva Fellowship (JCI-2012-13232 to

**Fig. 4.** Recruited endogenous bone-marrow cells preferentially fuse with Müller glial cells. (a, b) Representative images from retinal flat mounts (a) and sections (b) of NMDA-damaged R26Y/BM$^{CRE\text{-}RFP}$ chimeric mice, showing co-localization of YFP$^+$ hybrids (green) with the glial marker GS (red). Cell nuclei were counterstained with DAPI (blue). Higher magnification images are shown in the white boxes. Scale bar: A, 10 μm; B, 50 μm. (c) Schematic representation of the experimental plan. We used GFAP-Cre/BM$^{R26Y}$ chimeric mice, generated by replacing the BM of GFAP-Cre mice with the BM of donor transgenic mice carrying the R26Y allele. In GFAP-Cre mice, Cre recombinase expression is under the control of the glial-specific GFAP promoter. BMCs from R26Y donors will become YFP$^+$ following Cre-mediated excision of the floxed-STOP codon. Consequently, YFP expression will only be present as a result of fusion events between R26Y BMCs and Cre-expressing glial cells. We injected NMDA in the right eyes of GFAP-Cre/BM$^{R26Y}$ chimeric mice. Left eyes were injected with PBS, as a control. Mice were sacrificed 24 hpi and 3 wpi for immunostaining and FACS analysis. (d) Percentage of YFP$^+$ hybrids relative to total retinal cells in PBS-injected (CTR) and NMDA-damaged (NMDA) retinae of GFAP-Cre/BM$^{R26Y}$ chimeric mice, as analyzed by FACS 24 hpi. Values represent means ± S.E.M. (n = 7). Statistical analysis is based on unpaired Student's t-test ($p = 0.2029^{ns}$). (e) Representative immunostaining images of retinal sections from PBS- (CTR) and NMDA-injected retinae of chimeric GFAP-Cre/BM$^{R26Y}$ mice, sacrificed 24 hpi. Co-localization of YFP$^+$ hybrids (green) and GS (red) is indicated by the yellow arrows. Nuclei were counterstained with DAPI (blue). Higher magnification images (from the areas enclosed by the white boxes) are shown in the left panels. Sections from at least three different mice were analyzed (n = 3). (onl, outer nuclear layer; inl, inner nuclear layer) Scale bar: 25 μm.

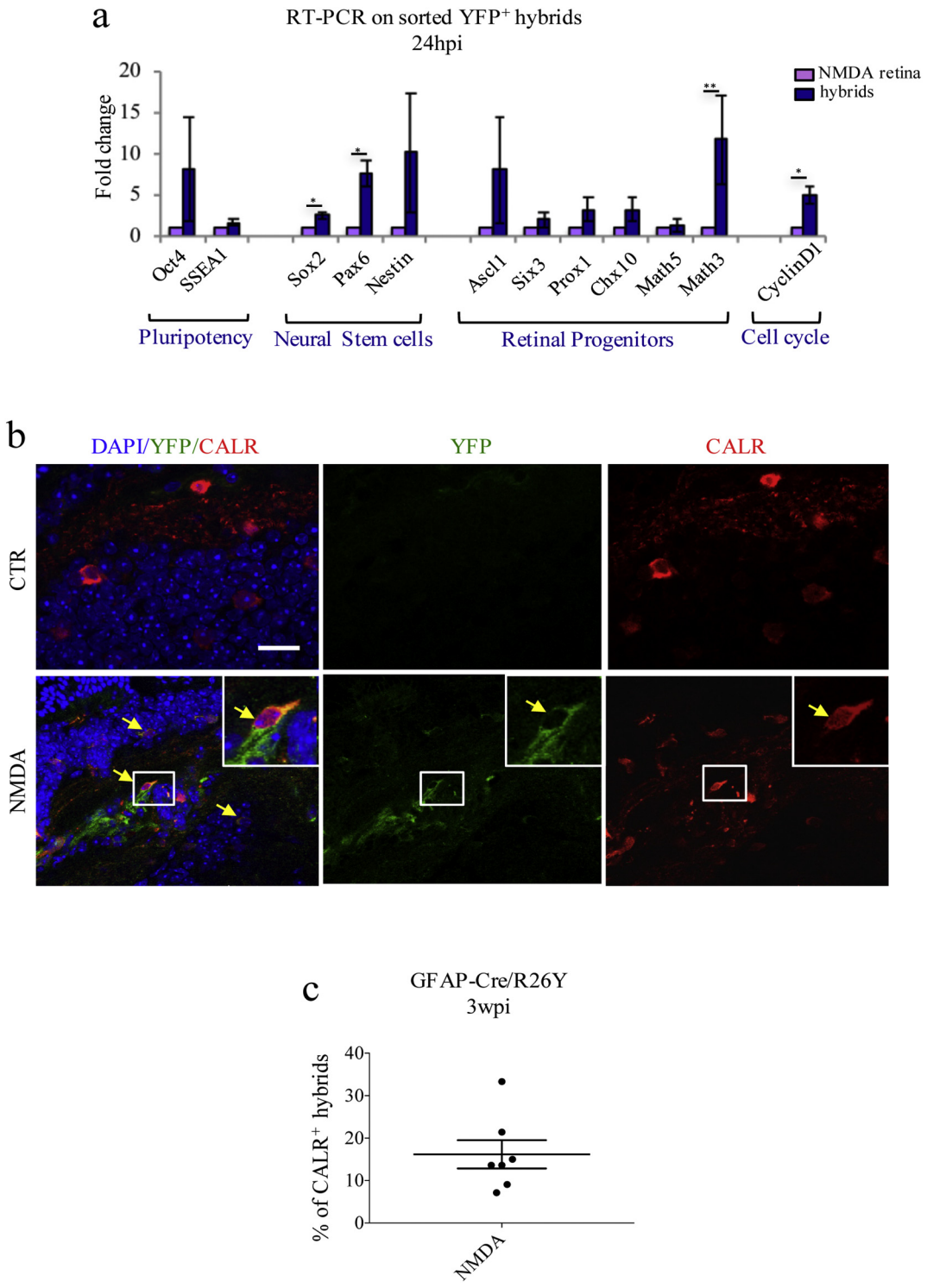


**Fig. 5.** BMC-MGC hybrids undergo reprogramming and can differentiate into CALR$^+$ cells in the long term. (a) RT-PCR analysis of YFP$^+$ hybrids FACS-sorted from NMDA-damaged retinae of GFAP-Cre/BM$^{R26Y}$ mice, 24 hpi. Transcript levels of are expressed as fold-changes relative to hybrids-depleted retinae (NMDA retina). Values represent means ± S.E.M. ($n \geq 3$). Statistical analysis is based on unpaired Student's *t*-test (Oct4, $p = 0.3266^{ns}$; SSEA1, $p = 0.3205^{ns}$, Sox2, $p = 0.0139^{*}$; Pax, $p = 0.0153^{*}$; Nestin, $p = 0.2728^{ns}$; Ascl1, $p = 0.3358^{ns}$; Six3, $p = 0.3822^{ns}$; Prox1, $p = 0.2247^{ns}$; Chx10, $p = 0.2774^{ns}$; Math5, $p = 0.7969^{ns}$; Math3, $p = 0.0048^{**}$; CyclinD1, $p = .0237^{*}$). (b) Representative immunostaining images of retinal flat mounts from undamaged (CTR) and damaged (NMDA) GFAP-Cre/BM$^{R26Y}$ chimeric mice, 3 wpi ($n = 3$). Yellow arrows show co-localization of YFP$^+$ hybrids (green) with CALR (red). Scale bar: 20 μm. (c) Percentages of YFP$^+$/CALR$^+$ hybrids relative to total of YFP$^+$ hybrids counted in random fields of retinal flat mounts from GFAP-Cre/BM$^{R26Y}$ chimeric mice, 3 wpi ($n = 3$).

D.S.), Boehringer Ingelheim Foundation Fellowship (BIF fellowship to G.S.), Subprograma estatal de Formación del Ministerio de Economía y Competitividad ref. BES-2015-075802 (to M.P.) and ref. BES-2015-075805 (to S.B.P.), and the co-finance of Fondo Social Europeo (FSE, BES-2015-072802). We also acknowledge support of the CERCA Programme (Generalitat de Catalunya), and of the Spanish Ministry of Economy and Competitiveness, "Centro de Excelencia Severo Ochoa".

## Author Contributions

G.S., M.P., and S.B.P. designed and performed the experiments, analyzed data, and wrote the paper. D.S. supervised some experiments. U. D.V. handled mice. M.P.C. analyzed the data, wrote the manuscript, and supervised the project.

## Conflict of Interest

The authors declare no competing financial interests.

## Acknowledgements

We would like to thank the PRBB animal facility, and the Histology, Microscopy, and Flow Cytometry Facilities of the CRG/UPF. We thank Wassim Altharche-Xifro, Neus Romo, and Elisa Pedone for their suggestions with respect to both the manuscript and the experiments. We also thank Ruben Sebastian-Perez, Marie Victoire Neguembor and Elena Tandardini for critical reading of the manuscript. Finally, we thank Alberto Oliveri for his help with the graphical design of the figures.

## Appendix A. Supplementary data

Supplementary data to this article can be found online at https://doi.org/10.1016/j.ebiom.2018.02.023.

## References

Aiuti, A., Webb, I.J., Bleul, C., Springer, T., Gutierrez-Ramos, J.C., 1997. The chemokine SDF-1 is a chemoattractant for human CD34+ hematopoietic progenitor cells and provides a new mechanism to explain the mobilization of CD34+ progenitors to peripheral blood. J. Exp. Med. 185, 111–120.

Altarche-Xifro, W., Di Vicino, U., Munoz-Martin, M.I., Bortolozzi, A., Bove, J., Vila, M., Cosma, M.P., 2016. Functional rescue of dopaminergic neuron loss in Parkinson's disease mice after transplantation of hematopoietic stem and progenitor cells. EBioMedicine 8, 83–95.

Alvarez-Dolado, M., Pardal, R., Garcia-Verdugo, J.M., Fike, J.R., Lee, H.O., Pfeffer, K., Lois, C., Morrison, S.J., Alvarez-Buylla, A., 2003. Fusion of bone-marrow-derived cells with Purkinje neurons, cardiomyocytes and hepatocytes. Nature 425, 968–973.

Berninger, B., Costa, M.R., Koch, U., Schroeder, T., Sutor, B., Grothe, B., Gotz, M., 2007. Functional properties of neurons derived from in vitro reprogrammed postnatal astroglia. J. Neurosci. 27, 8654–8664.

Blackshaw, S., Harpavat, S., Trimarchi, J., Cai, L., Huang, H., Kuo, W.P., Weber, G., Lee, K., Fraioli, R.E., Cho, S.H., Yung, R., Asch, E., Ohno-Machado, L., Wong, W.H., Cepko, C.L., 2004. Genomic analysis of mouse retinal development. PLoS Biol. 2, E247.

Bringmann, A., Pannicke, T., Biedermann, B., Francke, M., Iandiev, I., Grosche, J., Wiedemann, P., Albrecht, J., Reichenbach, A., 2009. Role of retinal glial cells in neurotransmitter uptake and metabolism. Neurochem. Int. 54, 143–160.

Cheng, M., Qin, G., 2012. Progenitor cell mobilization and recruitment: SDF-1, CXCR4, alpha4-integrin, and c-kit. Prog. Mol. Biol. Transl. Sci. 111, 243–264.

Chiquet, C., Dkhissi-Benyahya, O., Cooper, H.M., 2005. Calcium-binding protein distribution in the retina of strepsirhine and haplorhine primates. Brain Res. Bull. 68, 185–194.

Close, J.L., Liu, J., Gumuscu, B., Reh, T.A., 2006. Epidermal growth factor receptor expression regulates proliferation in the postnatal rat retina. Glia 54, 94–104.

Davies, P.S., Powell, A.E., Swain, J.R., Wong, M.H., 2009. Inflammation and proliferation act together to mediate intestinal cell fusion. PLoS One 4, e6530.

DeLeve, L.D., Wang, X., Wang, L., 2016. VEGF-sdf1 recruitment of CXCR7+ bone marrow progenitors of liver sinusoidal endothelial cells promotes rat liver regeneration. Am. J. Physiol. Gastrointest. Liver Physiol. 310, G739–46.

Enzmann, V., Lecaude, S., Kruschinski, A., Vater, A., 2017. CXCL12/SDF-1-dependent retinal migration of endogenous bone marrow-derived stem cells improves visual function after pharmacologically induced retinal degeneration. Stem Cell Rev. 13, 278–286.

Fausett, B.V., Goldman, D., 2006. A role for alpha1 tubulin-expressing Muller glia in regeneration of the injured zebrafish retina. J. Neurosci. 26, 6303–6313.

Fazel, S., Cimini, M., Chen, L., Li, S., Angoulvant, D., Fedak, P., Verma, S., Weisel, R.D., Keating, A., Li, R.K., 2006. Cardioprotective c-kit+ cells are from the bone marrow and regulate the myocardial balance of angiogenic cytokines. J. Clin. Invest. 116, 1865–1877.

Ferrari, G., Cusella-De Angelis, G., Coletta, M., Paolucci, E., Stornaiuolo, A., Cossu, G., Mavilio, F., 1998. Muscle regeneration by bone marrow-derived myogenic progenitors. Science 279, 1528–1530.

Fischer, A.J., Reh, T.A., 2001. Muller glia are a potential source of neural regeneration in the postnatal chicken retina. Nat. Neurosci. 4, 247–252.

Fischer, A.J., Reh, T.A., 2002. Exogenous growth factors stimulate the regeneration of ganglion cells in the chicken retina. Dev. Biol. 251, 367–379.

Fischer, A.J., Reh, T.A., 2003. Potential of Muller glia to become neurogenic retinal progenitor cells. Glia 43, 70–76.

Gallina, D., Palazzo, I., Steffenson, L., Todd, L., Fischer, A.J., 2016. Wnt/beta-catenin-signaling and the formation of Muller glia-derived progenitors in the chick retina. Dev. Neurobiol. 76, 983–1002.

Goldman, D., 2014. Muller glial cell reprogramming and retina regeneration. Nat. Rev. Neurosci. 15, 431–442.

Goto, H., Tomono, Y., Ajiro, K., Kosako, H., Fujita, M., Sakurai, M., Okawa, K., Iwamatsu, A., Okigaki, T., Takahashi, T., Inagaki, M., 1999. Identification of a novel phosphorylation site on histone H3 coupled with mitotic chromosome condensation. J. Biol. Chem. 274, 25543–25549.

Guo, Z., Zhang, L., Wu, Z., Chen, Y., Wang, F., Chen, G., 2014. In vivo direct reprogramming of reactive glial cells into functional neurons after brain injury and in an Alzheimer's disease model. Cell Stem Cell 14, 188–202.

Hattori, K., Heissig, B., Tashiro, K., Honjo, T., Tateno, M., Shieh, J.H., Hackett, N.R., Quitoriano, M.S., Crystal, R.G., Rafii, S., Moore, M.A., 2001. Plasma elevation of stromal cell-derived factor-1 induces mobilization of mature and immature hematopoietic progenitor and stem cells. Blood 97, 3354–3360.

Heinrich, C., Gascon, S., Masserdotti, G., Lepier, A., Sanchez, R., Simon-Ebert, T., Schroeder, T., Gotz, M., Berninger, B., 2011. Generation of subtype-specific neurons from postnatal astroglia of the mouse cerebral cortex. Nat. Protoc. 6, 214–228.

Heinrich, C., Bergami, M., Gascon, S., Lepier, A., Vigano, F., Dimou, L., Sutor, B., Berninger, B., Gotz, M., 2014. Sox2-mediated conversion of NG2 glia into induced neurons in the injured adult cerebral cortex. Stem Cell Rep. 3, 1000–1014.

Heins, N., Malatesta, P., Cecconi, F., Nakafuku, M., Tucker, K.L., Hack, M.A., Chapouton, P., Barde, Y.A., Gotz, M., 2002. Glial cells generate neurons: the role of the transcription factor Pax6. Nat. Neurosci. 5, 308–315.

Jackson, K.A., Majka, S.M., Wang, H., Pocius, J., Hartley, C.J., Majesky, M.W., Entman, M.L., Michael, L.H., Hirschi, K.K., Goodell, M.A., 2001. Regeneration of ischemic cardiac muscle and vascular endothelium by adult stem cells. J. Clin. Invest. 107, 1395–1402.

Jadhav, A.P., Roesch, K., Cepko, C.L., 2009. Development and neurogenic potential of Muller glial cells in the vertebrate retina. Prog. Retin. Eye Res. 28, 249–262.

Jiang, S.M., Zeng, L.P., Zeng, J.H., Tang, L., Chen, X.M., Wei, X., 2015. β-III-Tubulin: a reliable marker for retinal ganglion cell labeling in experimental models of glaucoma. Int. J. Ophthalmol. 8, 643–652.

Johansson, C.B., Youssef, S., Koleckar, K., Holbrook, C., Doyonnas, R., Corbel, S.Y., Steinman, L., Rossi, F.M., Blau, H.M., 2008. Extensive fusion of haematopoietic cells with Purkinje neurons in response to chronic inflammation. Nat. Cell Biol. 10, 575–583.

Jorstad, N.L., Wilken, M.S., Grimes, W.N., Wohl, S.G., Vandenbosch, L.S., Yoshimatsu, T., Wong, R.O., Rieke, F., Reh, T.A., 2017. Stimulation of functional neuronal regeneration from Muller glia in adult mice. Nature 548, 103–107.

Kale, S., Karihaloo, A., Clark, P.R., Kashgarian, M., Krause, D.S., Cantley, L.G., 2003. Bone marrow stem cells contribute to repair of the ischemically injured renal tubule. J. Clin. Invest. 112, 42–49.

Karl, M.O., Reh, T.A., 2010. Regenerative medicine for retinal diseases: activating endogenous repair mechanisms. Trends Mol. Med. 16, 193–202.

Karl, M.O., Hayes, S., Nelson, B.R., Tan, K., Buckingham, B., Reh, T.A., 2008. Stimulation of neural regeneration in the mouse retina. Proc. Natl. Acad. Sci. U. S. A. 105, 19508–19513.

Karow, M., Sanchez, R., Schichor, C., Masserdotti, G., Ortega, F., Heinrich, C., Gascon, S., Khan, M.A., Lie, D.C., Dellavalle, A., Cossu, G., Goldbrunner, R., Gotz, M., Berninger, B., 2012. Reprogramming of pericyte-derived cells of the adult human brain into induced neuronal cells. Cell Stem Cell 11, 471–476.

Kilkenny, C., Browne, W., Cuthill, I.C., Emerson, M., Altman, D.G., National Centre for the Replacement, R, Reduction of Amimals in, R, 2011. Animal research: reporting in vivo experiments—the ARRIVE guidelines. J. Cereb. Blood Flow Metab. 31, 991–993.

Kohno, H., Sakai, T., Kitahara, K., 2006. Induction of nestin, Ki-67, and cyclin D1 expression in Muller cells after laser injury in adult rat retina. Graefes Arch. Clin. Exp. Ophthalmol. 244, 90–95.

Kollet, O., Shivtiel, S., Chen, Y.Q., Suriawinata, J., Thung, S.N., Dabeva, M.D., Kahn, J., Spiegel, A., Dar, A., Samira, S., Goichberg, P., Kalinkovich, A., Arenzana-Seisdedos, F., Nagler, A., Hardan, I., Revel, M., Shafritz, D.A., Lapidot, T., 2003. HGF, SDF-1, and MMP-9 are involved in stress-induced human CD34+ stem cell recruitment to the liver. J. Clin. Invest. 112, 160–169.

Lagasse, E., Connors, H., Al-Dhalimy, M., Reitsma, M., Dohse, M., Osborne, L., Wang, X., Finegold, M., Weissman, I.L., Grompe, M., 2000. Purified hematopoietic stem cells can differentiate into hepatocytes in vivo. Nat. Med. 6, 1229–1234.

Lai, P., Li, T., Yang, J., Xie, C., Zhu, X., Xie, H., Ding, X., Lin, S., Tang, S., 2008. Upregulation of stromal cell-derived factor 1 (SDF-1) expression in microvasculature endothelial cells in retinal ischemia-reperfusion injury. Graefes Arch. Clin. Exp. Ophthalmol. 246, 1707–1713.

Lenkowski, J.R., Raymond, P.A., 2014. Muller glia: stem cells for generation and regeneration of retinal neurons in teleost fish. Prog. Retin. Eye Res. 40, 94–123.

Li, Y., Reca, R.G., Atmaca-Sonmez, P., Ratajczak, M.Z., Ildstad, S.T., Kaplan, H.J., Enzmann, V., 2006. Retinal pigment epithelium damage enhances expression of chemoattractants and migration of bone marrow-derived stem cells. Invest. Ophthalmol. Vis. Sci. 47, 1646–1652.

Lima E Silva, R., Shen, J., Hackett, S.F., Kachi, S., Akiyama, H., Kiuchi, K., Yokoi, K., Hatara, M. C., Lauer, T., Aslam, S., Gong, Y.Y., Xiao, W.H., Khu, N.H., Thut, C., Campochiaro, P.A., 2007. The SDF-1/CXCR4 ligand/receptor pair is an important contributor to several types of ocular neovascularization. FASEB J. 21, 3219–3230.

Livesey, F.J., Young, T.L., Cepko, C.L., 2004. An analysis of the gene expression program of mammalian neural progenitor cells. Proc. Natl. Acad. Sci. U. S. A. 101, 1374–1379.

Long, J.Z., Lackan, C.S., Hadjantonakis, A.K., 2005. Genetic and spectrally distinct in vivo imaging: embryonic stem cells and mice with widespread expression of a monomeric red fluorescent protein. BMC Biotechnol. 5, 20.

Lucas, D.R., Newhouse, J.P., 1957. The toxic effect of sodium L-glutamate on the inner layers of the retina. AMA Arch. Ophthalmol. 58, 193–201.
Maga, G., Hubscher, U., 2003. Proliferating cell nuclear antigen (PCNA): a dancer with many partners. J. Cell Sci. 116, 3051–3060.
Mocco, J., Afzal, A., Ansari, S., Wolfe, A., Caldwell, K., Connolly, E.S., Scott, E.W., 2014. SDF1-a facilitates Lin-/Sca1+ cell homing following murine experimental cerebral ischemia. PLoS One 9, e85615.
Mojumder, D.K., Wensel, T.G., Frishman, L.J., 2008. Subcellular compartmentalization of two calcium binding proteins, calretinin and calbindin-28 kDa, in ganglion and amacrine cells of the rat retina. Mol. Vis. 14, 1600–1613.
Nagashima, M., Barthel, L.K., Raymond, P.A., 2013. A self-renewing division of zebrafish Muller glial cells generates neuronal progenitors that require N-cadherin to regenerate retinal neurons. Development 140, 4510–4521.
Nervi, B., Link, D.C., Dipersio, J.F., 2006. Cytokines and hematopoietic stem cell mobilization. J. Cell. Biochem. 99, 690–705.
Newman, E., Reichenbach, A., 1996. The Muller cell: a functional element of the retina. Trends Neurosci. 19, 307–312.
Niu, W., Zang, T., Zou, Y., Fang, S., Smith, D.K., Bachoo, R., Zhang, C.L., 2013. In vivo reprogramming of astrocytes to neuroblasts in the adult brain. Nat. Cell Biol. 15, 1164–1175.
Nygren, J.M., Jovinge, S., Breitbach, M., Sawen, P., Roll, W., Hescheler, J., Taneera, J., Fleischmann, B.K., Jacobsen, S.E., 2004. Bone marrow-derived hematopoietic cells generate cardiomyocytes at a low frequency through cell fusion, but not transdifferentiation. Nat. Med. 10, 494–501.
Ooto, S., Akagi, T., Kageyama, R., Akita, J., Mandai, M., Honda, Y., Takahashi, M., 2004. Potential for neural regeneration after neurotoxic injury in the adult mammalian retina. Proc. Natl. Acad. Sci. U. S. A. 101, 13654–13659.
Orlic, D., Kajstura, J., Chimenti, S., Jakoniuk, I., Anderson, S.M., Li, B., Pickel, J., Mckay, R., Nadal-Ginard, B., Bodine, D.M., Leri, A., Anversa, P., 2001. Bone marrow cells regenerate infarcted myocardium. Nature 410, 701–705.
Osakada, F., Ooto, S., Akagi, T., Mandai, M., Akaike, A., Takahashi, M., 2007. Wnt signaling promotes regeneration in the retina of adult mammals. J. Neurosci. 27, 4210–4219.
Pasteels, B., Rogers, J., Blachier, F., Pochet, R., 1990. Calbindin and calretinin localization in retina from different species. Vis. Neurosci. 5, 1–16.
Pedone, E., Olteanu, V.A., Marucci, L., Munoz-Martin, M.I., Youssef, S.A., De Bruin, A., Cosma, M.P., 2017. Modeling dynamics and function of bone marrow cells in mouse liver regeneration. Cell Rep. 18, 107–121.
Petersen, B.E., Bowen, W.C., Patrene, K.D., Mars, W.M., Sullivan, A.K., Murase, N., Boggs, S. S., Greenberger, J.S., Goff, J.P., 1999. Bone marrow as a potential source of hepatic oval cells. Science 284, 1168–1170.
Pollak, J., Wilken, M.S., Ueki, Y., Cox, K.E., Sullivan, J.M., Taylor, R.J., Levine, E.M., Reh, T.A., 2013. ASCL1 reprograms mouse Muller glia into neurogenic retinal progenitors. Development 140, 2619–2631.
Priller, J., Flugel, A., Wehner, T., Boentert, M., Haas, C.A., Prinz, M., Fernandez-Klett, F., Prass, K., Bechmann, I., De Boer, B.A., Frotscher, M., Kreutzberg, G.W., Persons, D.A., Dirnagl, U., 2001. Targeting gene-modified hematopoietic cells to the central nervous system: use of green fluorescent protein uncovers microglial engraftment. Nat. Med. 7, 1356–1361.
Reichenbach, A., Bringmann, A., 2013. New functions of Muller cells. Glia 61, 651–678.
Ringuette, R., Atkins, M., Lagali, P.S., Bassett, E.A., Campbell, C., Mazerolle, C., Mears, A.J., Picketts, D.J., Wallace, V.A., 2016. A notch-Gli2 axis sustains hedgehog responsiveness of neural progenitors and Muller glia. Dev. Biol. 411, 85–100.
Rizvi, A.Z., Swain, J.R., Davies, P.S., Bailey, A.S., Decker, A.D., Willenbring, H., Grompe, M., Fleming, W.H., Wong, M.H., 2006. Bone marrow-derived cells fuse with normal and transformed intestinal stem cells. Proc. Natl. Acad. Sci. U. S. A. 103, 6321–6325.
Sahel, J.A., Albert, D.M., Lessell, S., 1990. Proliferation of retinal glia and excitatory amino acids. Ophtalmologie 4, 13–16.
Sanges, D., Romo, N., Simonte, G., Di Vicino, U., Tahoces, A.D., Fernandez, E., Cosma, M.P., 2013. Wnt/beta-catenin signaling triggers neuron reprogramming and regeneration in the mouse retina. Cell Rep. 4, 271–286.
Sanges, D., Simonte, G., Di Vicino, U., Romo, N., Pinilla, I., Nicolas, M., Cosma, M.P., 2016. Reprogramming Muller glia via in vivo cell fusion regenerates murine photoreceptors. J. Clin. Invest. 126, 3104–3116.
Siliprandi, R., Canella, R., Carmignoto, G., Schiavo, N., Zanellato, A., Zanoni, R., Vantini, G., 1992. N-methyl-D-aspartate-induced neurotoxicity in the adult rat retina. Vis. Neurosci. 8, 567–573.
Song, W.T., Zhang, X.Y., Xia, X.B., 2015. Atoh7 promotes the differentiation of Muller cells-derived retinal stem cells into retinal ganglion cells in a rat model of glaucoma. Exp. Biol. Med. 240, 682–690.
Srinivas, S., Watanabe, T., Lin, C.S., William, C.M., Tanabe, Y., Jessell, T.M., Costantini, F., 2001. Cre reporter strains produced by targeted insertion of EYFP and ECFP into the ROSA26 locus. BMC Dev. Biol. 1, 4.
Stadtfeld, M., Graf, T., 2005. Assessing the role of hematopoietic plasticity for endothelial and hepatocyte development by non-invasive lineage tracing. Development 132, 203–213.
Stone, J., Dreher, Z., 1987. Relationship between astrocytes, ganglion cells and vasculature of the retina. J. Comp. Neurol. 255, 35–49.
Su, Z., Niu, W., Liu, M.L., Zou, Y., Zhang, C.L., 2014. In vivo conversion of astrocytes to neurons in the injured adult spinal cord. Nat. Commun. 5, 3338.
Sucher, N.J., Lipton, S.A., Dreyer, E.B., 1997. Molecular basis of glutamate toxicity in retinal ganglion cells. Vis. Res. 37, 3483–3493.
Takeda, M., Takamiya, A., Jiao, J.W., Cho, K.S., Trevino, S.G., Matsuda, T., Chen, D.F., 2008. alpha-Aminoadipate induces progenitor cell properties of Muller glia in adult mice. Invest. Ophthalmol. Vis. Sci. 49, 1142–1150.
Taniguchi, H., He, M., Wu, P., Kim, S., Paik, R., Sugino, K., Kvitsiani, D., Fu, Y., Lu, J., Lin, Y., Miyoshi, G., Shima, Y., Fishell, G., Nelson, S.B., Huang, Z.J., 2011. A resource of Cre driver lines for genetic targeting of GABAergic neurons in cerebral cortex. Neuron 71, 995–1013.
Tao, Z., Zhao, C., Jian, Q., Gillies, M., Xu, H., Yin, Z.Q., 2016. Lin28B promotes Muller glial cell de-differentiation and proliferation in the regenerative rat retinas. Oncotarget 7, 49368–49383.
Thummel, R., Kassen, S.C., Enright, J.M., Nelson, C.M., Montgomery, J.E., Hyde, D.R., 2008. Characterization of Muller glia and neuronal progenitors during adult zebrafish retinal regeneration. Exp. Eye Res. 87, 433–444.
Todd, L., Volkov, L.I., Zelinka, C., Squires, N., Fischer, A.J., 2015. Heparin-binding EGF-like growth factor (HB-EGF) stimulates the proliferation of Muller glia-derived progenitor cells in avian and murine retinas. Mol. Cell. Neurosci. 69, 54–64.
Tucker, B.A., Park, I.H., Qi, S.D., Klassen, H.J., Jiang, C., Yao, J., Redenti, S., Daley, G.Q., Young, M.J., 2011. Transplantation of adult mouse iPS cell-derived photoreceptor precursors restores retinal structure and function in degenerative mice. PLoS One 6.
Turner, D.L., Cepko, C.L., 1987. A common progenitor for neurons and glia persists in rat retina late in development. Nature 328, 131–136.
Ueki, Y., Wilken, M.S., Cox, K.E., Chipman, L., Jorstad, N., Sternhagen, K., Simic, M., Ullom, K., Nakafuku, M., Reh, T.A., 2015. Transgenic expression of the proneural transcription factor Ascl1 in Muller glia stimulates retinal regeneration in young mice. Proc. Natl. Acad. Sci. U. S. A. 112, 13717–13722.
Vassilopoulos, G., Wang, P.R., Russell, D.W., 2003. Transplanted bone marrow regenerates liver by cell fusion. Nature 422, 901–904.
Wan, J., Zheng, H., Chen, Z.L., Xiao, H.L., Shen, Z.J., Zhou, G.M., 2008. Preferential regeneration of photoreceptor from Muller glia after retinal degeneration in adult rat. Vis. Res. 48, 223–234.
Wang, X., Willenbring, H., Akkari, Y., Torimaru, Y., Foster, M., Al-Dhalimy, M., Lagasse, E., Finegold, M., Olson, S., Grompe, M., 2003. Cell fusion is the principal source of bone-marrow-derived hepatocytes. Nature 422, 897–901.
Watanabe, T., Raff, M.C., 1988. Retinal astrocytes are immigrants from the optic nerve. Nature 332, 834–837.
Webster, M.K., Cooley-Themm, C.A., Barnett, J.D., Bach, H.B., Vainner, J.M., Webster, S.E., Linn, C.L., 2017. Evidence of BrdU-positive retinal neurons after application of an Alpha7 nicotinic acetylcholine receptor agonist. Neuroscience 346, 437–446.
Weimann, J.M., Charlton, C.A., Brazelton, T.R., Hackman, R.C., Blau, H.M., 2003a. Contribution of transplanted bone marrow cells to Purkinje neurons in human adult brains. Proc. Natl. Acad. Sci. U. S. A. 100, 2088–2093.
Weimann, J.M., Johansson, C.B., Trejo, A., Blau, H.M., 2003b. Stable reprogrammed heterokaryons form spontaneously in Purkinje neurons after bone marrow transplant. Nat. Cell Biol. 5, 959–966.
Yao, K., Qiu, S., Tian, L., Snider, W.D., Flannery, J.G., Schaffer, D.V., Chen, B., 2016. Wnt regulates proliferation and neurogenic potential of Muller glial cells via a Lin28/let-7 miRNA-dependent pathway in adult mammalian retinas. Cell Rep. 17, 165–178.
Young, R.W., 1985. Cell differentiation in the retina of the mouse. Anat. Rec. 212, 199–205.
Yu, J., Li, M., Qu, Z., Yan, D., Li, D., Ruan, Q., 2010. SDF-1/CXCR4-mediated migration of transplanted bone marrow stromal cells toward areas of heart myocardial infarction through activation of PI3K/Akt. J. Cardiovasc. Pharmacol. 55, 496–505.
Zhuo, L., Theis, M., Alvarez-Maya, I., Brenner, M., Willecke, K., Messing, A., 2001. hGFAP-cre transgenic mice for manipulation of glial and neuronal function in vivo. Genesis 31, 85–94.